南华盆地新元古代成冰纪成锰作用及其成矿背景

付勇[1, 2)]，郭川[1, 2)]

1)贵州大学资源与环境工程学院，贵阳，500025；
2)贵州大学喀斯特地质资源与环境教育部重点实验室，贵阳，500025

www.geojournals.cn/georev

内容提要：南华盆地成冰系大塘坡组锰矿是我国最重要的锰矿产出层位之一，它形成于成冰纪 Sturtian 冰川事件之后，其成矿背景及形成机理一直是研究的重点。在系统总结 Sturtian 冰川事件起始与结束时间、南华裂谷盆地结构演化及古气候演变等重大地质事件的最新研究进展的基础上，综合分析了南华盆地大型沉积型锰矿成矿作用过程与这些重大地质事件之间的联系。揭示了南华盆地 Sturtian 冰期的启动和结束与全球其他地区基本一致，分别发生在~717 Ma 和~660 Ma 之前。同时，对南华系大塘坡锰矿成矿时代进行了约束，大约形成于~660 Ma 之前。在新元古代中期 Rodinia 超大陆裂解作用的影响下，南华裂谷盆地内部发育一系列由同沉积断层控制的地垒—地堑次级盆地。沿同沉积断层运移的热液流体为大塘坡锰矿的形成提供了大量的成矿物质，并控制着大塘坡锰矿的发育分布。化学蚀变指数（*CIA*）、锂同位素（δ^7Li）及锇同位素组成[$n(^{187}Os)/n(^{188}Os)$]等风化指标显示，南华盆地 Sturtian 冰期晚期至间冰期大塘坡期早期的气候为寒冷干燥，随后转为温暖湿润并很快变为寒冷干燥。至大塘坡中晚期，气候逐渐由寒冷干燥恢复至温暖湿润，并一直保持至大塘坡晚期。整体来看，Sturtian 冰期结束后，南华盆地表层海水逐渐氧化，深部沉积水体出现局部间歇式氧化环境，裂陷阶段热液和陆源输入的 Mn^{2+} 被氧化为 MnO_2 发生沉淀，并在底部伴随着有机质的埋藏及早期成岩作用而最终形成菱锰矿。

关键词：Sturtian 冰期；古气候；大塘坡锰矿；新元古代；南华盆地

新元古代是地球演化过程中的一个重要时期，伴随着强烈和广泛的冰川作用（Hoffman et al., 1998）、真核生物扩张（Sahoo et al., 2016）及条带状铁建造（BIF）的再现（Cox et al., 2013）等。这些重大地质事件与当时的气候、海水化学性质及板块构造运动等密切相关，长期以来一直是地球科学研究的重点。其中成冰纪发生了两次全球范围的冰川事件（即 Sturtian 和 Marinoan 冰期），分别对应着华南地区的江口冰期和南沱冰期（赵彦彦等，2011；张启锐等，2016），这两次冰期事件很大程度上改变了当时的大陆风化作用，并进一步造成了海洋的化学性质和氧化还原状态的显著变化（Hoffman et al., 2017）。华南地区的这两次冰期之间发生了大塘坡间冰期，对应着我国重要的成锰期，在此期间华南地区形成了丰富的沉积型锰矿床。多年勘探显示，华南地区南华系地层中发育多个大中型沉积型锰矿床（付勇等，2014），如贵州大塘坡（周琦等，2013；Yu Wenchao et al., 2019；张予杰等，2020）、重庆秀山（凌云等，2016；Ma Zhixin et al., 2019；赵志强等，2019）、湖南湘潭（史富强等，2016）等，其中锰矿石主要赋存在大塘坡组第一段（或相当层位）的黑色岩系中，使得黔、湘、渝等地区成为我国最重要的锰矿产地之一。由于大塘坡组锰矿具有重要的经济价值和科学意义，使得南华纪时期与其形成密切相关的 Sturtian 冰川事件、盆地演化、古气候及海洋氧化还原状态等内容一直是研究的热点（Li Chao et al., 2012；杜远生等，2015；齐靓等，2015；周琦等，2016；Lan Zhongwu et al., 2020）。

1 南华盆地 Sturtian 冰期时限及南华系锰矿成矿时代

目前 Sturtian 冰期时限及沉积矿床的形成年龄

注：本文为国家自然科学基金资助项目（编号：41763006、41673060）、中国地质调查局中国矿产地质志项目（编号：DD20190379）及贵州省人才基地资助项目（编号：RCJD2018-21）的成果。
收稿日期：2021-03-15；改回日期：2021-05-28；网络首发：2021-06-20；责任编辑：刘志强。Doi：10.16509/j.georeview.2021.06.031
作者简介：付勇，男，1980年生，博士，副教授，主要从事沉积学、沉积地球化学、沉积矿床学研究；Email：byez1225@126.com。

主要通过一系列的间接定年方法(如 Rb-Sr、Sm-Nd、锆石 U-Pb 法等),主要通过对冰期地层、含矿层系或相邻地层中的火山灰或成岩矿物来实现,但这些间接定年方法受其测试对象稀缺性和自身性质的制约,而使其应用存在很大的局限性(Rasmussen, 2005)。相比之下,Re-Os 定年方法能直接限定富有机质沉积岩(如黑色页岩)的沉积年龄(Cohen et al., 1999; Kendall et al., 2004; 李超等, 2014; Fu Yong et al., 2016; 王富良等, 2016)。近期研究显示,在后期成岩作用(如热成熟、低变质作用等)过程中,黑色页岩中的 Re-Os 体系仍能保持封闭,即不会发生 Re 和 Os 元素的丢失或获取(Creaser et al., 2002; Rooney et al., 2010; 李超等, 2014),这使得 Re-Os 定年方法被广泛用来限定前寒武系沉积地层的沉积年龄(Rooney et al., 2010; Zhu Bi et al., 2013; Tripathy and Singh, 2015)。

1.1 Sturtian 冰期启动时间

Sturtian 冰期地层在全球范围内广泛分布,但典型的冰期沉积主要发育在澳大利亚、纳米比亚、加拿大、中国南部、阿曼和蒙古等地区(Hoffman and Li, 2009; 赵彦彦和郑永飞, 2011; Hoffman et al., 2017)。这次冰期对应着华南地区的江口冰期,代表沉积为江口群(长安组+富禄组)或两界河组与铁丝坳组(Lan Zhongwu et al., 2014; 汪正江等, 2015)。近年来,针对成冰纪冰川事件的期次、起始与结束时间及全球对比,前人通过冰期沉积或相邻地层中的火山灰等开展了大量的研究工作,并取得了一系列的进展(图 1 和表 1)。其中,Lan Zhongwu 等(2014)获得了桂北地区丹洲群顶部凝灰质粉砂岩和湖北宜昌地区莲沱组顶部凝灰岩的 SIMS U-Pb 年龄,分别为 716.1 ± 3.4 Ma 和 715.9 ± 2.8 Ma; Lan Zhongwu 等(2015)获得的湖北宜昌地区莲沱组顶部凝灰岩 SIMS U-Pb 年龄为 714 ± 8 Ma;覃永军等(2015)获得的黔东南地区下江群顶界 U-Pb 年龄为 717 Ma;Jiang Zhuo-Fei 等(2016)获得的川西地区开建桥组顶部凝灰岩夹层的 SHRIMP 和 LA-ICP-MS U-Pb 年龄分别为 715.0 ± 9.8 Ma 和 718.8 ± 9.4 Ma;Song Gaoyuan 等(2017)获得的湘西地区板溪群顶部碎屑锆石的 LA-ICP-MS U-Pb 年龄为 714.6 ± 5.2 Ma;蔡娟娟等(2018)获得的桂北地区长安组底部冰成杂砾岩碎屑锆石的 LA-ICP-MS U-Pb 最小加权平均年龄为 719.6 ± 6.1 Ma; Lan Zhongwu 等(2020)获得的长安组之下拱洞组顶部的 CA-ID-IRMS 锆石 U-Pb 年龄(720.16 ± 1.42 Ma),并通过 Monte Carlo 模拟将华南地区 Sturtian 冰期的发生时间限定在 717.61 ± 1.65 Ma。因此,华南地区 Sturtian 冰期的发生时间应为~717 Ma。

针对 Sturtian 冰期的起始时间,国外学者也开展了大量的研究。其中,Fanning 和 Link(2004)获得的劳伦西亚 Grand Canyon 地区 Pocatello 组 Scout Mountain 段之上冰碛岩斑状流纹岩中岩浆锆石的 SHRIMP U-Pb 年龄为 717 ± 6 Ma; Bowring 等(2007)获得的阿曼 Ghubrah 冰碛岩中火山碎屑凝灰岩中的锆石 TIMS U-Pb 年龄为 713.7 ± 0.5 Ma,这代表了最接近阿曼斯图特冰期起始时间的年龄数据,但由于取样点位于混积岩之中,因此阿曼斯图特冰期的起始时间应早于 713 Ma。Macdonald 等(2010, 2018)获得了加拿大西北部地区 Mount Harper 群底部及其之下地层火山灰高分辨率锆石 TIMS 年龄,将加拿大地盾斯图特冰期的起始时间限定在 717.4 ± 0.1 Ma 和 716.9 ± 0.4 Ma。因此,这些年龄数据显示,不同纬度不同大陆上的 Sturtian 冰期可能是一次同时启动的、快速的全球性事件,其发生的时间应为 ~ 717 Ma(图 1;Macdonald et al., 2010; Lan Zhongwu et al., 2020)。

1.2 Sturtian 冰期结束时间及南华盆地南华系锰矿成矿时代

(1) Sturtian 冰期结束时间。由于华南地区 Sturtian 冰期地层(如富禄组、铁丝坳组或古城组)中尚未发现用于高精度定年的同沉积火山岩,因此 Sturtian 冰期结束的时间通常由上覆间冰期地层大塘坡组底部的凝灰岩层限定。Zhou Chuanming 等(2004)获得的华南贵州东部松桃地区大塘坡组底部凝灰岩中锆石的 ID-TIMS U-Pb 年龄为 662.9 ± 4.3 Ma,之后通过 CA-ID-IRMS U-Pb 法将之修正为 659.96 ± 0.46 Ma(Zhou Chuanming et al., 2020),但由于其采样部位处于大塘坡组底部位,说明 Sturtian 冰期结束时间应发生于之前。随后,尹崇玉等(2006)也获得了贵州东部松桃地区黑水溪剖面大塘坡组底部凝灰岩 SHRIMP U-Pb 年龄为 667.3 ± 9.9 Ma。之后,不同学者进一步开展了一系列 Sturtian 冰期结束时间的定年工作。例如,Zhang Shihong 等(2008)获得的华南湖北西部地区紧邻南沱组下部湘锰组(大塘坡组相当层位)凝灰岩层中锆石的 SHRIMP U-Pb 年龄为 654.5 ± 3.8 Ma;余文超等(2016b)和 Yu Wenchao 等(2017)获得的华南贵州东部松桃地区将军山剖面和寨浪沟剖面大塘坡组底部含锰页岩层锆石的 LA-ICP-MS U-Pb 年龄

表 1 新元古代 Sturtian 冰期起始和结束年龄汇编

Table 1 Compilation of chronometric dates for the onset and termination of the Neoproterozoic Sturtian glaciation

样品产地	方法	年龄(Ma)	岩石(矿物)类型和位置	资料来源
华南桂北地区	LA-ICP-MS U-Pb	719.6±6.1	南华系长安组底部冰成杂砾岩中的碎屑锆石	蔡娟娟等,2018
华南广西罗城县	CA-ID-IRMS U-Pb	717.61±1.65	拱洞组顶部黑色页岩中凝灰岩层中的锆石	Lan Zhongwu et al., 2020
劳伦西亚 Grand Canyon 地区	SHRIMP U-Pb	717±6	Pocatello 组 Scout Mountain 段之上冰碛岩斑状流纹岩中的岩浆锆石	Fanning and Link, 2004
加拿大西北部 Mackenzie 山脉	TIMS U-Pb	717.4±0.1	Mount Harper 上部冰碛岩之下火山杂岩中的锆石	Macdonald et al., 2010
	TIMS U-Pb	716.5±0.2	Mount Harper 上部冰碛岩内部角砾状凝灰岩中的锆石	
华南广西罗城县	SIMS U-Pb	716.1 ± 3.4	长安组之下凝灰质砂岩中的锆石	Lan Zhongwu et al., 2014
华南广西三江县	SIMS U-Pb	715.9 ± 2.8		
华南湖南西部四都坪	LA-ICP-MS U-Pb	714.6 ± 5.2	板溪群五强溪组顶部细粒砂岩中的锆石	Song Gaoyuan et al., 2017
阿曼北部 Sultanate	U-Pb	711.8±1.6	Huqf 超群中 Sturtian 下部 Ghubrah 冰碛岩的凝灰质杂砂岩中的锆石	Allen et al., 2002
阿曼北部 Jebel 地区	TIMS U-Pb	711.5±0.3	Ghubrah 冰碛岩中火山碎屑凝灰岩中的锆石	Bowring et al., 2007
美国 Idaho 中部	SHRIMP U-Pb	699±3	基底(BigCreek 群)之上的流纹岩中的锆石	Lund et al., 2003
劳伦西亚大陆	TIMS U-Pb	688.6+9.5/−6.2	可与 Yukon 的 Hyland 群进行对比的长石火山碎屑岩中的锆石	Ferri et al., 1999
美国 Idaho 南部	SHRIMP U-Pb	686±4	Pocatello 组 ScoutMoutain 段冰碛岩之下的长英质斑杂角砾岩的锆石	Fanning and Link, 2008
美国 Idaho 中部	SHRIMP U-Pb	685±7	Edwardsburg 组杂砾岩(冰碛岩)火山岩夹层中的锆石	Evans et al., 1997
		684±4		
华南贵州松桃	SHRIMP U-Pb	667.3±9.9	大塘坡组底部凝灰岩中的锆石	尹崇玉等,2006
美国 Pocatello 南部 Porteuf Narrow 地区	SHRIMP U-Pb	667±5	Scout Mountain 段冰期沉积杂砾岩顶部帽酸盐岩之上 20 m,但第二层似帽碳酸盐岩之下的再沉积凝灰岩层中的锆石	Fanning and Link, 2004
华南贵州松桃将军山	LA-ICP-MS U-Pb	664.2±2.4	大塘坡组底部凝灰岩层中的锆石	余文超等,2016
澳大利亚南部	CA-ID-TIMS U-Pb	663.03 ± 0.11	紧邻 Appila (Sturt) 组冰碛岩之上 Wilyerpa 组中火山灰层的锆石	Cox et al., 2018
华南贵州东部地区	ID-TIMS U-Pb	662.9±4.3	铁丝坳和大塘坡组之间夹凝灰岩层的锆石	Zhou Chuanming et al., 2004
华南贵州松桃	LA-ICP-MS U-Pb	662.7±6.4	大塘坡组底部含锰页岩层中凝灰岩夹层的锆石	Yu Wenchao et al., 2017
Laurentia Mackenzie Mountains 地区	Re-Os	662.4±3.9	Hay Creek 群 Twitya 组底部黑色页岩	Rooney et al., 2014
华南桂西北地区	U-Pb	661±7	南华系大塘坡组底部凝灰岩中的锆石	高林志等,2013
华南贵州西南地区	CA-ID-TIMS U-Pb	660.98 ± 0.74	贵州东南部地区大塘坡组底部含锰页岩层中的锆石	Rooney et al., 2020
华南贵州东北地区	Re-Os	660.6 ± 3.9	贵州东北部距铁丝坳组顶部 3 米的黑色页岩	Rooney et al., 2020
华南贵州道坨	Re-Os	660.6 ± 7.5	大塘坡组底部含锰黑色页岩	裴浩翔等,2017
苏联乌拉尔地区	TIMS U-Pb	660±15	Laplandian 冰碛岩之上火山灰层的锆石	Semikhatov (1991
华南贵州东部地区	CA-ID-IRMS U-Pb	659.96±0.46	铁丝坳和大塘坡组之间夹凝灰岩层的锆石	Zhou Chuanming et al., 2020
澳大利亚南部	SHRIMP U-Pb	659.7±5.3	紧邻 Appila (Sturt) 组冰碛岩之上 Wilyerpa 组中火山灰层的锆石	Fanning and Link, 2008
华南贵州松桃将军山	SIMS U-Pb	659.3±2.4	大塘坡组底部含锰页岩层凝灰岩中的锆石	Wang Ping et al., 2019
蒙古 Tuva—Mongolia	Re-Os	659.0±4.5	Taishir 组底部黑色页岩	Rooney et al., 2015
华南湖南西部地区	CA-ID-TIMS U-Pb	658.97 ± 0.76	大塘坡组底部含锰页岩层中的锆石	Rooney et al., 2020
华南贵州松桃将军山	CA-ID-TIMS U-Pb	658.8 ± 0.5	大塘坡组底部盖帽碳酸盐岩中的锆石	Zhou Chuanming et al., 2019
澳大利亚南部	SIMS U-Pb	658	Umberatan 群 Enorama 组黑色页岩 Marino Arkose 段中的碎屑锆石	Fanning and Link, 2006
中国湖北宜昌	LA-ICP-MS U-Pb	658.1±2.6	大塘坡组底部凝灰岩层中的锆石	李明龙等,2021
澳大利亚 Adelaide Rift Complex 地区	Re-Os	657.2±5.4	Appila (Sdturt) 组冰碛岩之上的 Tapley Hill 组底部 Tindelpina 段黑色页岩	Kendall et al., 2006
华南湖南西部地区	CA-ID-TIMS U-Pb	657.17 ± 0.78	大塘坡组底部含锰页岩层中的锆石	Rooney et al., 2020
中国湖北西部吉首地区	SHRIMP U-Pb	654.5±3.8	紧邻南沱组下部的湘锰组中凝灰岩层的锆石	Zhang Sihong et al., 2008

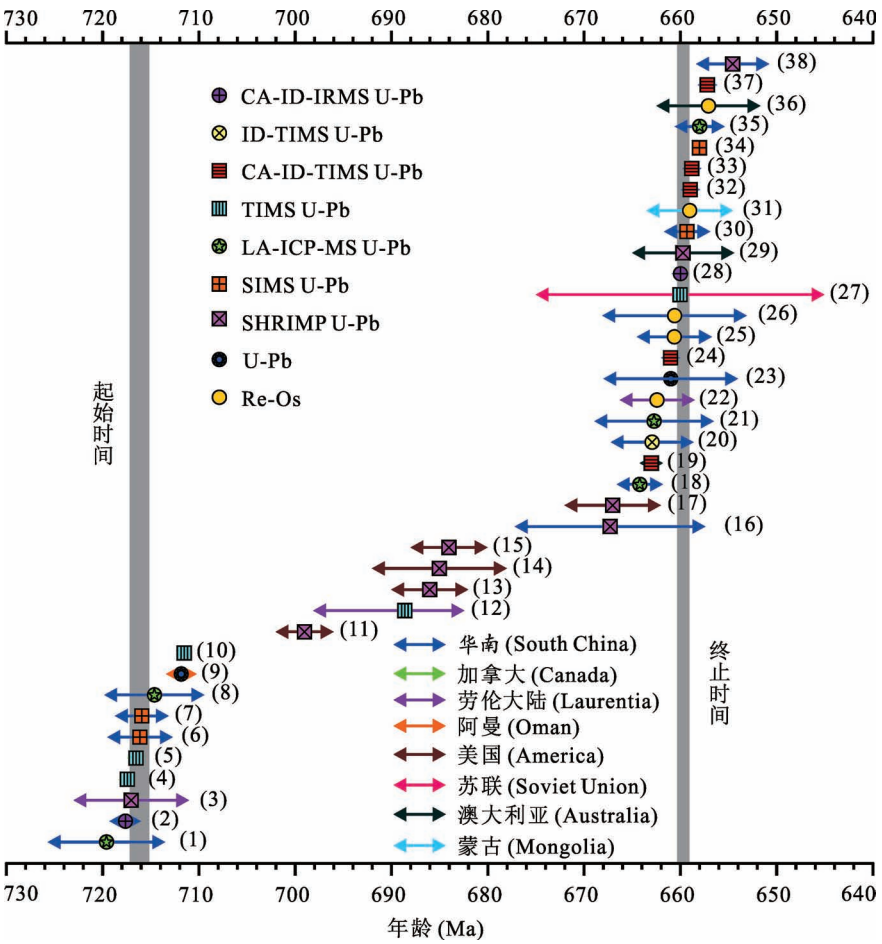

图 1 新元古代 Sturtian 冰期起始和结束年龄分布图

Fig. 1 The ages of the onset and termination of the Neoproterozoic Sturtian glaciation

数据来源:1—蔡娟娟等,2018;2—Lan Zhongwu et al., 2020;3, 17—Fanning and Link, 2004;4, 5—Macdonald et al., 2010;6, 7—Lan Zhongwu et al., 2014;8—Song Gaoyuan et al., 2017;9—Allen et al., 2002;10—Bowring et al., 2007;11—Lund et al., 2003;12—Ferri et al., 1999;13, 29—Fanning and Link, 2008;14, 15—Evans et al., 1997;16—尹崇玉等,2006;18—余文超等,2016b;19—Cox et al., 2018;20—Zhou Chuanming et al., 2004;21—Yu Wenchao et al., 2017;22—Rooney et al., 2014;23—高林志等,2013;24, 25 32, 37—Rooney et al., 2020;26—裴浩翔等,2017;27—Semikhatov, 1991;28—Zhou Chuanming et al., 2020;30—Wang Dan et al., 2019;31—Rooney et al., 2015;33—Zhou Chuanming et al., 2019;34—Fanning and Link, 2006;35—李明龙等,2021;36—Kendall et al., 2006;38—Zhang Sihong et al., 2008

Data are compiled from: 1—Cai Juanjuan et al., 2018&; 2—Lan Zhongwu et al., 2020; 3, 17—Fanning and Link, 2004; 4, 5—Macdonald et al., 2010; 6, 7—Lan Zhongwu et al., 2014; 8—Song Gaoyuan et al., 2017; 9—Allen et al., 2002; 10—Bowring et al., 2007; 11—Lund et al., 2003; 12—Ferri et al., 1999; 13, 29—Fanning and Link, 2008; 14, 15—Evans et al., 1997; 16—Yi Chongyu et al., 2006&; 18—Yu Wenchao et al., 2016b&; 19—Cox et al., 2018; 20—Zhou Chuanming et al., 2004; 21—Yu Wenchao et al., 2017; 22—Rooney et al., 2014; 23—Gao Linzhi et al., 2013&; 24, 25 32, 37—Rooney et al., 2020; 26—Pei Haoxiang et al., 2017&; 27—Semikhatov, 1991; 28—Zhou Chuanming et al., 2020; 30—Wang Ping et al., 2019; 31—Rooney et al., 2015; 33—Zhou Chuanming et al., 2019; 34—Fanning and Link, 2006; 35—Li Minglong et al., 2021&; 36—Kendall et al., 2006; 38—Zhang Shihong et al., 2008

分别为 664.2 ± 2.4 Ma 和 662.7 ± 6.2 Ma;Zhou Chuanming 等(2019)获得的华南云南东部地区大塘坡组底部盖帽白云岩凝灰岩层锆石的 CA-ID-TIMS U-Pb 年龄为 658.8 ± 0.5 Ma。最近,Rooney 等(2020)获得了贵州东南部地区和湖南西部地区大塘坡组底部含锰页岩层凝灰岩中锆石的 CA-ID-TIMS U-Pb 年龄,分别为 660.98 ± 0.74 Ma、658.97 ± 0.76 Ma、657.17 ± 0.78 Ma,其中 660.98 ± 0.74 Ma 为最接近大塘坡组底界的年龄。同时,Rooney 等(2020)还获得了贵州东北部距铁丝坳组顶部 3 m 的黑色页岩的 Re-Os 年龄为 660.6 ± 3.9 Ma,也进一步证实了富有机质沉积岩 Re-Os 年龄方法的可靠性。在华南湖北恩施地区,李明龙等(2021)获得的大塘坡组底部凝灰岩锆石的 LA-ICP-MS U-Pb 年龄为 658.1 ± 2.6 Ma。这些年龄数据在误差范围内完全一致,因此华南 Sturtian 冰期结束应发生在 ~660 Ma 前。

世界其他地区也获得了与华南地区类似的年龄,也进一步限定了 Sturtian 冰期结束的时间。例如,劳伦大陆获得的 Mackenzie Mountains 地区 Hay Creek 群 Twitya 组底部黑色页岩的 Re-Os 年龄为 662.4 ± 3.9 Ma(Rooney et al., 2014);前苏联乌拉尔地区 Laplandian 冰碛岩之下火山灰层锆石的 TIMS U-Pb 年龄为 660 ± 15 Ma(Semikhatov, 1991);澳大利亚南部地区紧邻 Appila(Sturt)组冰碛岩之上 Wilyerpa 组中火山灰层锆石的 CA-ID-TIMS U-Pb 年龄和 SIMS U-Pb 年龄分别为 663.03 ± 0.11 Ma(Cox et al., 2018)和 659.7±5.3 Ma(Fanning and Link, 2008);澳大利亚 Adelaide Rift Complex 地区 Appila

(Sdturt) 组冰碛岩之上的 Tapley Hill 组底部 Tindelpina 段黑色页岩的 Re-Os 年龄为 657.2 ± 5.4 Ma (Kendall et al., 2006); 蒙古 Tuva—MongoliaTaishir 组底部黑色页岩的 Re-Os 年龄为 659.0 ± 4.5 Ma(Rooney et al., 2015)。这些年龄与华南地区获得的年龄在误差范围内完全一致(图 1),因此,全球范围内 Sturtian 冰期的结束可能也是一个等时事件,其应发生在~660 Ma 之前,其持续时间约为 57 Ma (Rooney et al., 2014; Zhou Chuanming et al., 2019; Rooney et al., 2020)。

(2)南华盆地南华系锰矿成矿时代。由于 Sturtian 冰期结束的时限主要通过上覆大塘坡组底部凝灰岩和富有机质沉积岩(如黑色页岩)获得,这些年龄也对南华盆地南华系锰矿成矿时代进行了限定。近期,裴浩翔等(2017)获得的贵州东部道坨锰矿大塘坡组一段含锰黑色页岩的 Re-Os 同位素等时线年龄为 660.6 ± 7.5 Ma;Wang Dan 等(2019)获得的贵州东部松桃将军山剖面大塘坡组底部含锰页岩层凝灰岩中锆石的 SIMS U-Pb 年龄为 659.3 ± 2.4 Ma。这些年龄数据在误差范围内是一致的,因此结合前人报道的年龄数据可将南华盆地南华系锰矿限定在~ 660 Ma,该年龄可对该时期南华盆地甚至全球范围内的成矿地质事件提供很好的年龄约束,同时能为全球对比研究体统很好的年龄框架。

2　南华纪南华裂谷盆地结构演化

已有研究显示,南华裂谷盆地的形成与演化与 Rodinia 超大陆的裂解密切相关(王剑等, 2001; 杜远生等, 2018)。其中,Rodinia 超大陆的形成于中元古代末期(1300~900 Ma)的全球范围造山运动,这次构造运动几乎波及所有的大陆板块 (Hoffman, 1991; Li et al., 2008)。随后,新元古代时期(~750 Ma)发生了全球性的裂谷作用,导致 Rodinia 超大陆发生裂解,并最终在 600 Ma 完全解体(Li et al., 2008; Zhao Guochun et al., 2018; Wang Wei et al., 2020)。在 Rodinia 超大陆的形成—裂解过程中,扬子板块和华夏板块在 830 Ma 发生碰撞形成华南板块和江南造山带(王自强等, 2012; 孙海清等, 2013; 赵军红等, 2015; Li Qiwei and Zhao Junhong, 2020),并自 820 Ma 开始发生多次幕式大陆裂解作用(Wang Jian and Li Zhengxiang, 2003)。在此背景下,扬子板块内形成了以南华裂谷盆地为代表的沿东南方向展布的裂谷系统(王孝磊等, 2004; 杜远生等, 2015; Zhao Guochun et al., 2018),同时南华裂谷盆地内部也发育一系列由同沉积断层控制的地垒—地堑次级盆地(图 2;周琦等, 2016)。

由于青白口纪(~800 Ma)第一次裂陷活动的作用,在湘西、黔东、桂北地区(江南构造带西段)分别沉积了一系列以深水沉积组合和火山岩及凝灰岩沉积为特征的板溪群、下江群、丹洲群(杜远生等, 2015)。随后,南华纪(~725 Ma)发生了第二次裂陷活动,在湘黔边界地区沉积了大塘坡组以黑色泥质岩系为特征的深水沉积(图 3;Zhang Shihong et al., 2008)。而震旦纪(~635 Ma)发生了第三次裂陷活动,在江南构造带东侧形成了以硅质泥质岩系等深水沉积为特征的震旦系—奥陶系地层。整体来看,扬子地块东南缘裂谷盆地(I 级)可划分为武陵次级裂谷盆地、天柱—怀化隆起及雪峰次级裂谷盆地 3 个 II 级结构单元,它们可进一步识别出间隔分布的 III 级地堑与地垒结构,如溪口—小茶园次级地堑盆地、松桃—石阡次级地堑盆地、万山—岑巩次级地堑盆地及黎平—从江次级地堑盆地(图 2;周琦等, 2016)。在这些地堑盆地内,大塘坡组沉积厚度自盆地中心向盆地边缘逐渐降低(图 3)。另一方面,由黔东地区向鄂西地区大塘坡组厚度逐渐降低,岩相组合在区域上也表现出明显的差异性,二分性逐渐消失(旷红伟等, 2019)。

3　南华纪南华盆地风化作用记录

“雪球地球”假说认为,新元古代成冰纪冰川事件之后,地球迅速转为温室气候条件,并同时伴随着强烈的化学风化作用过程(Hoffman et al., 1998; Hoffman and Schrag, 2002)。前人研究显示,大陆风化作用对海洋营养物质的输入有着非常重要的影响,并进一步制约着海水的氧化还原状态,如高营养物质输入会导致海洋表层海水高的初始生产力和富有机质页岩的沉积(Yeasmin et al., 2017; Huang Taiyu et al., 2019; Li Chao et al., 2020)。已有研究显示,南华盆地大塘坡组底部(或一段)锰矿的形成受沉积水柱氧化还原状态的制约(何志威等, 2014; Wu Chengquan et al., 2016; 余文超等, 2020)。为了明确大塘坡组(或相当层位)下部含锰岩系及黑色页岩形成时期海洋南华盆地的氧化还原状态,前人采用一系列地球化学指标开展了大量的研究工作,如元素地球化学(朱祥坤等, 2013; 何志威等, 2014; Wu Chengquan et al., 2016; 赵志强等, 2019)、碳同位素(Chen Xi et al., 2008; 裴浩翔等, 2020)、硫同位素(Li Chao et al., 2012; 张飞飞

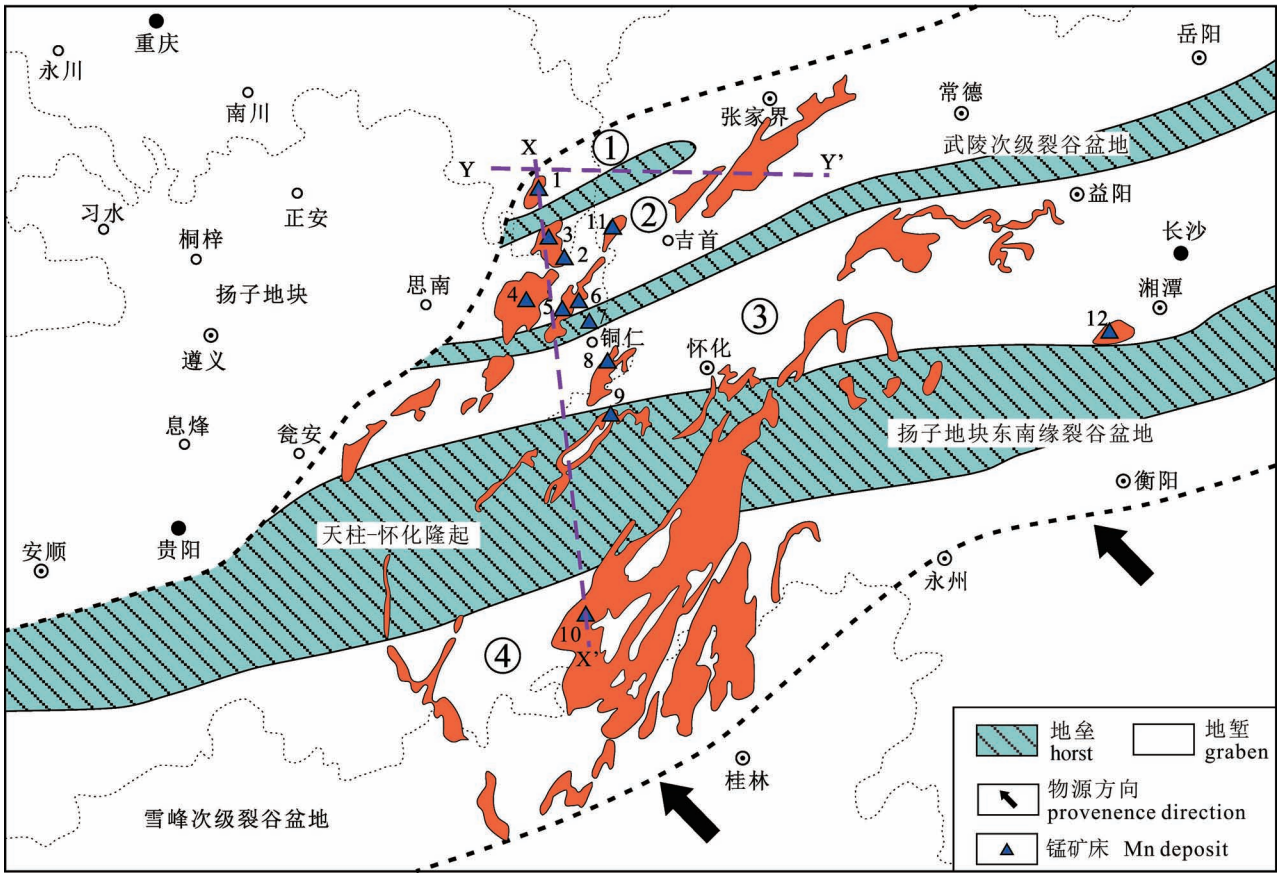

图 2 扬子地块东南缘裂谷盆地结构示意图及主要锰矿(剖面)分布图(修改自杜远生等, 2015)

Fig. 2 The tectonic architecture of rift basin of southeastern Yangtze Block and distribution map of Mn deposits (modified from Du Yuansheng et al. 2015&)

1—重庆秀山小茶园锰矿;2—重庆秀山盐井沟剖面;3—重庆秀山笔架山锰矿;4—贵州松桃道坨锰矿;5—贵州松桃两界河锰矿;6—贵州松桃西溪堡锰矿;7—贵州江口桃映剖面;8—贵州铜仁万山石竹溪锰矿床;9—贵州新晃板桥剖面;10—贵州从江八当锰矿点;11—湖南花垣民乐锰矿;12—湖南湘潭锰矿床。① 溪口—小茶园次级地堑盆地;② 松桃—石阡次级地堑盆地;③ 万山—岑巩次级地堑盆地;④ 黎平—从江次级地堑盆地

1—Xiaochayuan Mn deposit, Xiushan, Chongqing; 2—Yanjinggou Section, Xiushan, Chongqing; 3—Bijiashan Mn deposit, Xiushan, Chongqing; 4—Daotuo Mn desposit, Daotuo, Guizhou; 5—Liangjiehe Mn Deposit, Songtao, Guizhou; 6—Xixibao Mn deposit, Songtao, Guizhou; 7—Taoying Section, Jiangkou, Guizhou; 8—Shizhuxi Mn deposit, Wanshan, Tongren, Guizhou; 9—Banqiao Section, Xinhuang, Guizhou; 10—Badang Mn deposit, Congjiang, Guizhou; 11—Minle Mn deposit, Huayuan, Hunan; 12—Xiangtan Mn deposit, Hunan. ① Xikou—Xiaochayuan sub-graben basin; ② Songtao—Shiqian sub-graben basin; ③ Wanshan—Cenggong sub-graben basin; ④ Liping—Congjiang sub-graben basin

等, 2013; Wang Ping et al., 2019)、铁组分(Li Chao et al., 2012; Ma Zhixin et al., 2019)、氮同位素(Wei Wei et al., 2016)、锶-钕同位素(Yu Wenchao et al., 2016; 余文超等, 2016a)、钼同位素(Cheng Meng et al., 2018; Ye Yuntao et al., 2018; Tan Zhaozhao et al., 2021)、锂同位素(Wei Guangyi et al., 2020)等。结果显示,南华盆地沉积水体的氧化还原状态大致经历了 3 个阶段:① 冰期阶段主要为缺氧环境;② 成锰阶段主要为表层海水氧化、深部水体缺氧的分层海洋结构;③ 含锰岩系上覆黑色页岩沉积时期主要为缺氧环境(Li Chao et al., 2012; Cheng Meng et al., 2018; Tan Zhaozhao et al., 2021)。近期研究表明,冰期向间冰期转换阶段,大陆风化作用强度并非是迅速升高的,而是存在着多次短期的波动(Huang Kangjun et al., 2016; Li Chao et al., 2020)。针对南华纪南华盆地的大陆风化强度变化,前人已开展了化学蚀变指数(*CIA*;齐靓等, 2015; 李明龙等, 2019; Wang Ping et al., 2020)、锂同位素(δ^7Li)(Wei Guangyi et al., 2020)及锇同位素组成[$n(^{187}Os)/n(^{188}Os)$;裴浩翔等, 2017]等方面的研究,并取得一定的认识。

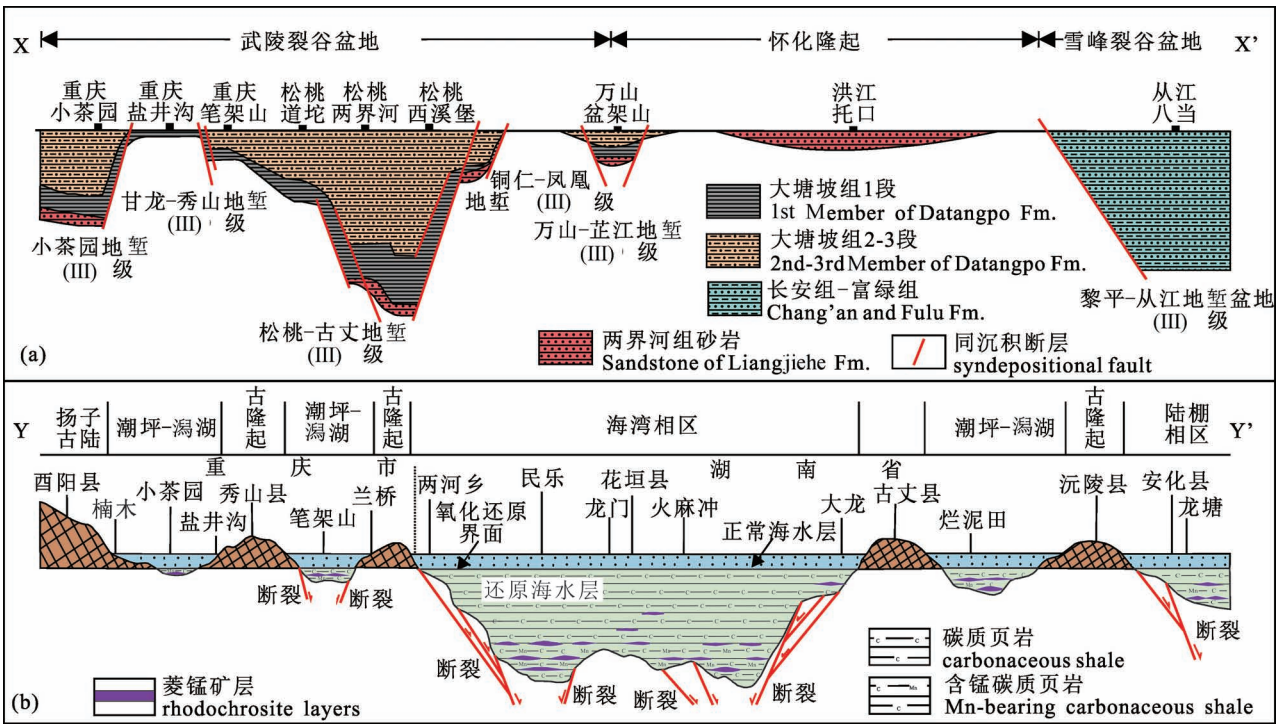

图 3 南华裂谷盆地南华纪两界河—大塘坡期盆地结构图(a,据周琦等, 2016 修改)和大塘坡期早期盆地结构图(b,据邹光均等, 2020 修改)

Fig. 3 The architecture of the Nanhua rift basin during the Lianghejie—Datangpo Age of the Nanhua Period (a, modified from Zhou Qi et al., 2016&) and during the early Datangpo Age (b, modified from Zou Guangjun et al., 2020&)

3.1 化学蚀变指数(*CIA*)和锂同位素(δ^7Li)

大陆化学风化作用过程主要受控于湿度和温度(Nesbitt and Young, 1982; Sheldon and Tabor, 2009)。在热带—亚热带潮湿气候背景下,高沉淀、高气温及高产率的酸性表层水体有利于强烈风化作用(Schoenborn and Fedo, 2011),可将砂质颗粒中的钾长石有效的转化为粘土矿物(Johnsson et al., 1991)。相比之下,在干旱和极地气候背景下,有限的沉淀作用及低温条件通常导致弱的化学风化作用,而且物理风化作用比化学风化作用更为有效,从而会形成化学上不成熟和相对欠风化的沉积物(Nesbitt and Young, 1989)。因此,Nesbitt 和 Young (1982) 提出的化学蚀变指数(Chemical index of alteration;*CIA*)可作为评估土壤和沉积物化学风化强度的指标,并具有古气候意义(Sheldon and Tabor, 2009; Zhai Lina et al., 2018; Wang Ping et al., 2020)。在不同气候条件下,风化搬运之后形成的沉积物具有不同的 *CIA* 值(Nesbitt and Young, 1989;冯连君等,2006)。例如,炎热湿润气候条件下形成的沉积物的 *CIA* 值通常为 80~100;温暖潮湿气候条件下一般为 70~80;寒冷干燥气候条件下形成的沉积物的 *CIA* 值为 55~70(冯连君等,2006)。但需要注意的是,沉积物的 *CIA* 值可能会受到物源组成、搬运过程中的水动力颠选作用及成岩期钾交代作用等因素的影响(McLennan, 1993; Bahlburg and Dobrzinski, 2011; 李明龙等, 2021)。相比之下,锂(Li)元素在自然界中主要以 Li^+ 离子形式存在,而且无化合价变化(苟龙飞等, 2017)。已有研究显示,大陆风化作用可造成 Li 同位素的最大分馏,但生物作用几乎不会造成 Li 同位素的分馏(苟龙飞等, 2017;Wei Guangyi et al., 2020)。在风化搬运过程中,轻的 Li 同位素(^{6}Li)会在次生粘土矿物中优先富集,而重的 Li 同位素(^{7}Li)则会被搬运至海洋中,从而导致海相自生粘土矿物通常具有比陆源风化产物更高的 δ^7Li 值(苟龙飞等, 2017;Wei Guangyi et al., 2020)。因此,海相细粒碎屑沉积岩中的 Li 同位素组成主要受控于其中陆源碎屑物质及海相自生粘土矿物的比例及其 Li 同位素组成。

李明龙等(2021)开展了鄂西走马地区钻孔 ZK701 南华系大塘坡组及相邻层段(下覆古城组和上覆南沱组)的 *CIA* 分析(图 4)。古城组顶部较低

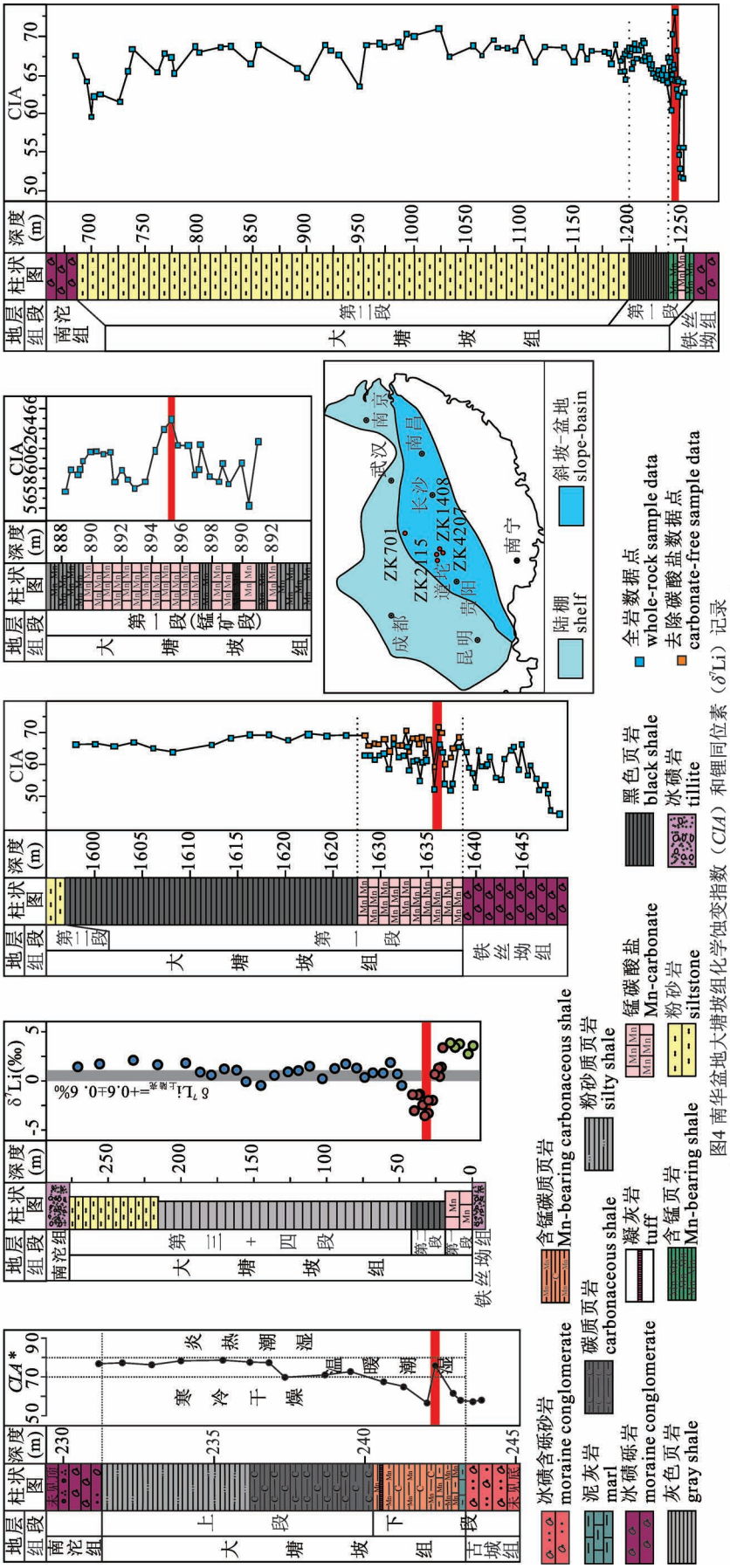

图4 南华盆地大塘坡组化学蚀变指数（*CIA*）和锂同位素（δ^7Li）记录

Fig. 4 The *CIA* and δ^7Li record of the Datangpo Formation of the Nanhua Basin

数据来源：ZK701-李明龙等，2021；道坨-Wei et al., 2020; ZK2115-Wang et al., 2020; ZK4207和ZK1408-齐靓等，2015

Data source: ZK701-Li Minglong et al., 2021&; Daotuo-Wei Guangyi et al., 2020; ZK2115-Wang Ping et al., 2020; ZK4207 and ZK1408-Qi Liang et al., 2015&

的 *CIA* 值（平均值为 57.6；n = 2）指示南华盆地 Sturtian 冰期晚期的气候条件仍为寒冷干燥，并一直持续至间冰期大塘坡期早期（*CIA* 平均值 = 59.1；n = 2）。随后，气候发生短暂的波动变化，先由寒冷干燥转为温暖湿润并很快变为寒冷干燥。至大塘坡中晚期，气候逐渐由寒冷干燥恢复至温暖湿润，并一直保持至大塘坡晚期。之后，可能受 Marinoan 冰期的影响，气候缓慢向寒冷干燥转变。这种变化趋势与鄂西走马地区钻孔 ZK701（李明龙等，2019）及黔东地区钻孔 ZK4207 与 ZK1408（齐靓等，2015）南华系的 *CIA* 值反映的气候演化基本一致（图 4）。由于大塘坡组底部锰矿层矿物相主要为碳酸锰，可能会对 *CIA* 计算产生较强的影响。为了消除这种影响，Wang Ping 等（2020）对黔东地区钻孔 ZK2115 锰矿层做了去碳酸盐组分处理。尽管处理前后的 *CIA* 值存在差异（处理过的样品值偏高），但在大塘坡组底部均存在一个低值区域，达到一个高值之后，再转为振荡的低值，并逐渐升高，指示气候变化与 ZK701 类似的趋势（图 4）。这种趋势在黔东地区道坨剖面大塘坡组的 δ^7Li 也有很好的响应（Wei Guangyi et al.,

2020)。整体来看,δ^7Li 值自大塘坡组底部表现出升高→降低→再升高的趋势,指示在大塘坡期早期寒冷干燥气候背景下大陆风化作用逐渐减弱,然后在气候转为温暖潮湿气候背景下大陆风化作用增强,并在气候再次转为寒冷干燥状态下大陆风化作用随之减弱(图 4)。随后,大塘坡期中晚期在温暖潮湿背景下大陆风化作用振荡变化,但维持一个较高的强度。

3.2　锇同位素组成[$n(^{187}Os)/n(^{188}Os)$]

在氧化性海水中,Re 和 Os 通常以 ReO^{-4} 和 $HOsO^{-5}$ 等高价态的稳定形式存在,在还原性海水中则会被还原成较难迁移的低价离子(Peucker-Ehrenbrink and Ravizza, 2000; Yamashita et al., 2007)。由于 Re、Os 的亲有机性,富有机质沉积岩在沉积过程中会吸附一定数量的低价 Re、Os 离子。另一方面,富有机质沉积岩(如黑色页岩)中 Os 元素主要为水成成因,从而导致富有机质沉积岩具有与同时期海水相同的 Os 同位素比值[即初始 $n(^{187}Os)/n(^{188}Os)$ 值;李超等, 2014]。因此,可通过 Re-Os 等时线年龄法获得富有机质沉积岩(如黑色页岩)的初始 $n(^{187}Os)/n(^{188}Os)$ 值,以此来约束同时期海水的 Os 同位素比值(Cohen et al., 1999; Peucker-Ehrenbrink and Ravizza, 2000; Cohen, 2004; Fu Yong et al., 2016; Wei Shuaichao et al., 2017; Rotich et al., 2020)。与 Sr 同位素一样,地质历史时期海水中的 Os 同位素组成并非保持不变,其变化非常剧烈(Cohen, 2004)。海水中的 Os 同位素组成主要有 3 个物源:①河流输入的高放射性的古老地壳风化 Os[现今河流的 $n(^{187}Os)/n(^{188}Os)$:1.4~1.6;Peucker-Ehrenbrink and Ravizza, 2000];②洋中脊热液蚀变输入的非放射性 Os[$n(^{187}Os)/n(^{188}Os)$ 约为 0.127;Esser and Turekian, 1993; Cohen, 2004];③宇宙尘埃带来的非放射性 Os[$n(^{187}Os)/n(^{188}Os)$ 约为 0.127; Shirey and Walker, 1998; Cohen, 2004]。整体来看,海水中的 Os 同位素主要是这 3 项来源的综合结果,地质历史时期突发性地质事件通常会改变不同端元的供给通量,从而可能造成海水 Os 同位素的相应波动(Ravizza and Turekian, 1989; Finlay et al., 2010)。现今正常海水的 $n(^{187}Os)/n(^{188}Os)$ 为 1.05~1.06,反映氧化风化状态下海水中的 Os 同位素组成主要来源于放射性陆壳的风化作用(Levasseur et al., 1998; Peucker-Ehrenbrink and Ravizza, 2000)。而太古宙海水的 $n(^{187}Os)/n(^{188}Os)$ 仅为 0.1~0.15(Anbar et al., 2007; Yang et al., 2009),则指示缺氧背景下海水中的 Os 同位素组成主要来源于洋中脊的热液蚀变作用(Hannah et al., 2004; Kendall et al., 2009)。因此,海水中 Os 同位素特征的变化可很好的用来示踪地质历史时期海洋和气候环境的演化特征(van Acken et al., 2013; Gibson et al., 2019; Rotich et al., 2020)。

尽管前寒武纪海水的 Os 同位素组成数据较少,其 $n(^{187}Os)/n(^{188}Os)$ 值整体表现出阶梯式增大的趋势(图 5),可能反映了大气氧气含量的幕式增加过程(Li Chao et al., 2012; Pufahl et al., 2014; Fan Haifeng et al., 2018; Cole et al., 2020; Uahengo et al., 2020; Wei Guangyi et al., 2021)。裴浩翔等(2017)获得的贵州道坨锰矿大塘坡组底部黑色页岩的初始 $n(^{187}Os)/n(^{188}Os)$ 值为 0.781,该值明显低于现今正常海水的 $n(^{187}Os)/n(^{188}Os)$ 值(图 5),指示大塘坡组底部沉积时期海水中 Os 同位素组成来源以海底洋中脊热液蚀变为主,这也与当时南华盆地广泛发育的裂谷活动相一致(杜远生等, 2015; 周琦等, 2016)。另一方面,较低的初始 $n(^{187}Os)/n(^{188}Os)$ 值也揭示了当时相对寒冷干燥气候背景下相对较弱的风化强度。Rooney 等(2020)总结了华南、蒙古及加拿大 Sturtian 冰期地层的 Os 同位素化学地层(图 6),可见 $n(^{187}Os)/n(^{188}Os)$ 值从 Sturtian 冰碛岩顶部的~1.4 逐渐降至距冰碛岩~2.5 m 的~0.4,随后逐渐升高。$n(^{187}Os)/n(^{188}Os)$ 值的变化特征揭示了大陆风化作用强度的变化趋势,即 Sturtian 冰期结束阶段大陆风化作用相对较强,进入间冰期之后,大陆风化作用可能明显减弱,随后再次增强(Li Chao et al., 2012)。Sturtian 冰期至间冰期大陆风化作用强度的变化特征与 Marinoan 冰期非常类似(Huang Kangjun et al., 2016)。

4　锰矿床成矿模式及南华盆地南华系锰矿成矿机理

4.1　锰矿床成矿模式

根据赋矿岩石类型的不同,我国锰矿床大致可分为有海相沉积型、火山—沉积型、碳酸盐岩中热水沉积型(或“层控”型)、与岩浆作用有关的热液型、受变质型及表生型 6 种类型(付勇等, 2014)。其中前 3 种类型主要为沉积型,中国与全球锰矿的分布和储量数据显示,这类锰矿床的工业价值最大,具有巨大的工业储量(付勇等, 2014; Maynard, 2010, 2014),其成矿过程与大气氧气含量、海洋氧化还原

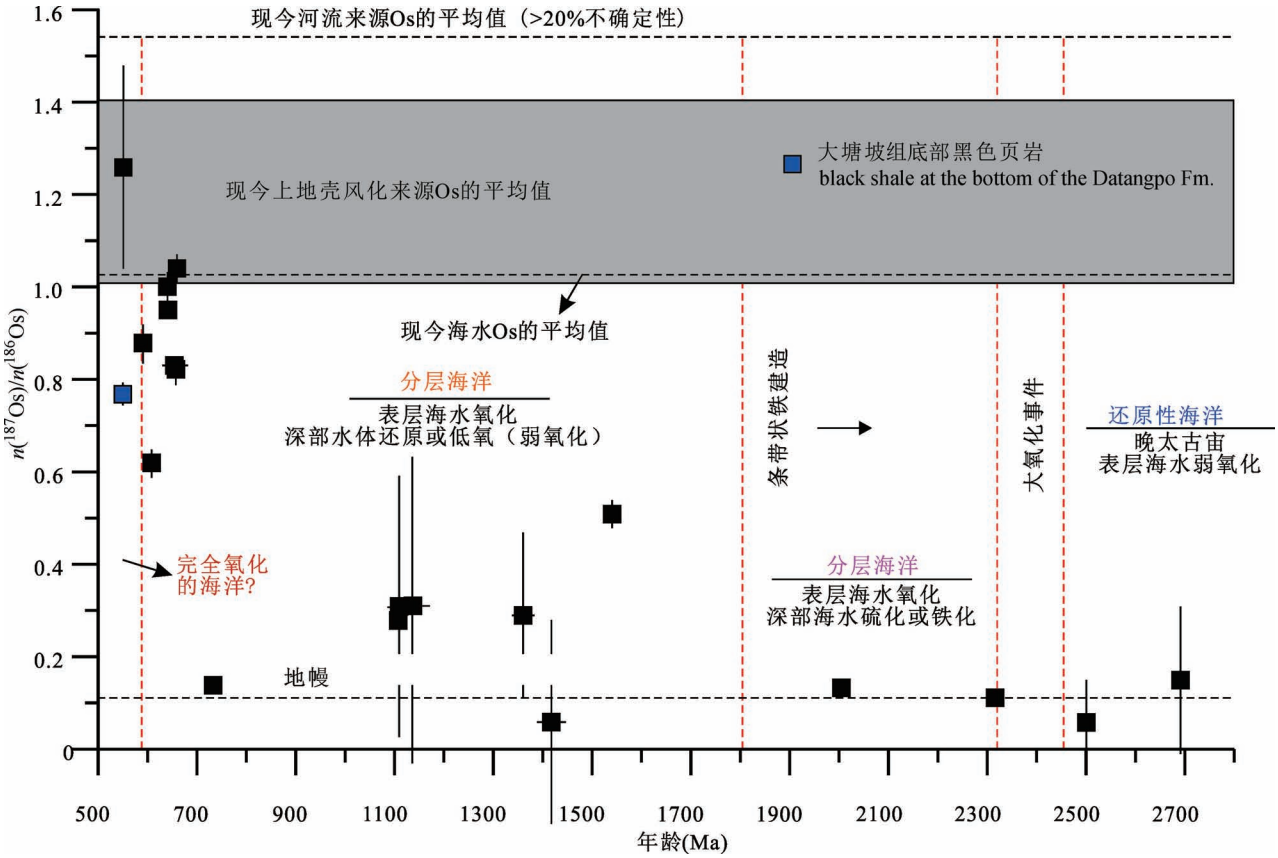

图 5 前寒武纪富有机质沉积岩和准同生—早期成岩黄铁矿的初始$n(^{187}Os)/n(^{188}Os)$值

Fig. 5 The initial $n(^{187}Os)/n(^{188}Os)$ of the Precambrian organic-rich sedimentary rocks and syndepositional—early diagenetic pyrite

引用数据来源于 Kendall et al., 2009、Rooney et al., 2010, 2011、裴浩翔等, 2017

Data are compiled from Kendall et al., 2009, Rooney et al., 2010, 2011 and Pei Haoxiang et al., 2017&

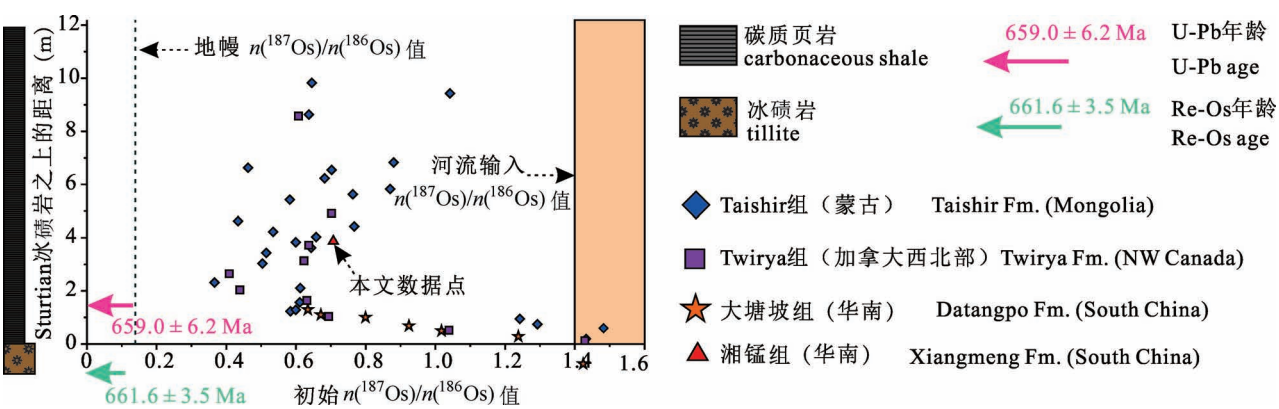

图 6 Sturtian 冰期结束后海水的 Os 同位素化学地层(修改自 Rooney et al., 2020)

Fig. 6 The composite Os isotope chemostratigraphy of the post-Sturtian successions (modified from Rooney et al., 2020)

引用数据来源于/Data from: Peucker-Ehrenbrink and Ravizza, 2000、Meisel et al., 2001、Rooney et al., 2014, 2015

状态及盆地类型等密切相关(Roy, 2006;付勇等, 2014)。针对沉积型锰矿床,目前国内外学者基于大量的实例研究提出了两种较为流行的锰矿成因模式:① 富锰缺氧海水中直接沉淀成矿(图 7a);② 成岩孔隙水中转化成矿(图 7b, c, d;董志国等, 2020)。

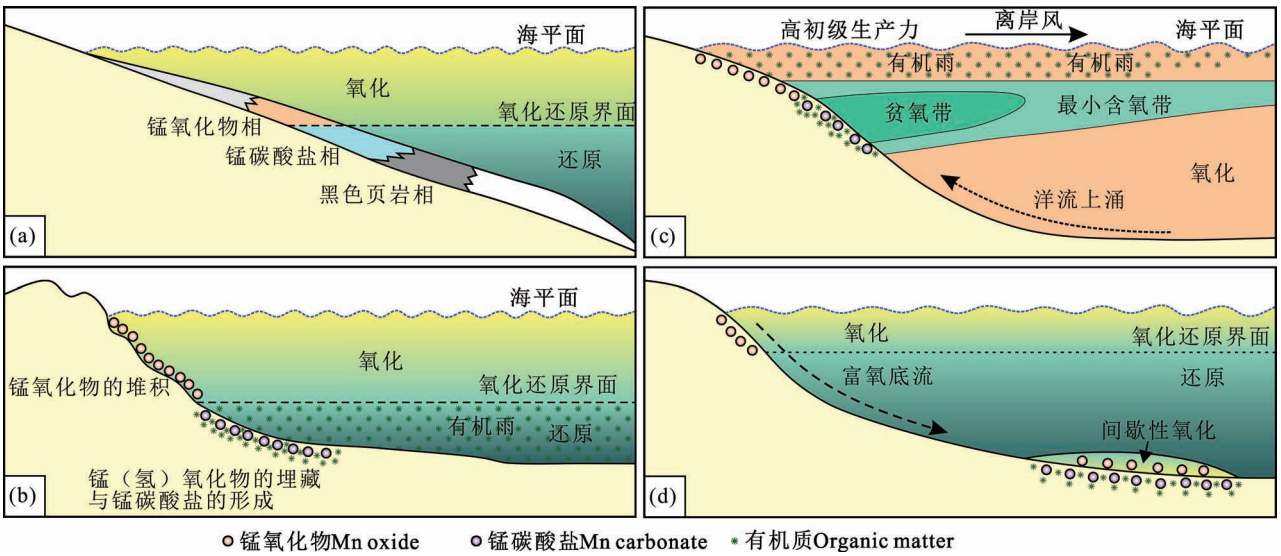

图 7 沉积型锰矿床主要成矿模式图

Fig. 7 The main metallogenic models of sedimentary manganese deposits

修改自/modified from: Force and Cannon, 1988; Huckriede and Meischner, 1996; Roy, 2006; Maynard, 2014

(1)富锰缺氧海水中直接沉淀成矿。锰是一种对氧化还原敏感的变价元素,其存在的形式主要受体系的 Eh—pH 条件控制(Roy, 2006)。在氧化水体中,锰主要以氧化物(Mn_2O_3)沉淀的形式存在;在还原性水体中,则主要以溶解态 Mn^{2+} 离子形式存在(Krauskopf, 1957)。在现代海洋缺氧水体(如开放海洋的最小含氧带或局限海洋分层水体的深部缺氧带)中 Mn^{2+} 相对集中,但大量实例研究和实验模拟显示,现代海洋缺氧水体的 Mn^{2+} 浓度并不足以沉淀出碳酸锰($MnCO_3$)矿物(Mucci, 2004; 王霄等, 2018)。另一方面,虽然铁与锰的化学性质比较类似,由于 $Mn^{2+}/Mn(OH)_3$ 的还原电位比 $Fe^{2+}/Fe(OH)_3$ 高(Lu Zunli et al., 2010),在适当的还原条件下铁和锰可发生分离(Krauskopf, 1957)。但大量的研究实例显示,沉积型锰矿床中并不存在明显的铁锰分带现象(Maynard, 2010)。因此,富锰缺氧海水中直接沉淀成矿模式还有待进一步的论证。

(2)成岩孔隙水中转化成矿。这种成矿模式主要包括 3 个阶段:① Mn^{2+} 离子在还原性缺氧水体中的富集;② 在氧化还原界面之上,运移过来的 Mn^{2+} 离子被氧化形成锰氧化物(或氢氧化物)发生沉淀;③随着上覆沉积物的堆积,沉积物—水界面之下逐渐演变为一个还原的微环境,早期沉积的锰氧化物(或氢氧化物)被微生物还原成 Mn^{2+} 离子,其与孔隙水中的碳酸根(CO_3^{2-})离子结合形成碳酸锰(即菱锰矿)发生沉淀(Roy, 2006; Maynard, 2014)。大量的研究实例显示,这种成矿模式主要发生在具氧化还原分层结构的盆地中(Roy, 2006; Maynard, 2014; 董志国等, 2020; 余文超等, 2020)。其中海洋的化学性质分层结构可形成于多种环境,如与极端地质事件(如冰川事件等;图 7b)有关的水体循环受限、最小氧化带的扩张(图 7c)及季节性富氧底流的输入(图 7d)等(Force and Cannon, 1988; Li Chao et al., 2012; Maynard, 2014)。近年来,越来越多的学者认为,在沉积型锰矿床形成过程中微生物可能也起着非常重要的作用(Fan Delian et al., 1999; Yu Wenchao et al., 2019)。

4.2　南华盆地南华系锰矿成矿机理

在元古宙时期,地球大气圈逐渐发生氧化,并对地球表层环境、海洋化学条件和元素循环过程等产生了深远的影响(Kump, 2008; Lyons et al., 2014; Cole et al., 2020)。大量的研究显示,大气圈氧气含量的增加并不是一个渐进的过程,而是在两次快速的增氧之后才达到现今的水平(Canfield, 2005; Lyons et al., 2014)。它们分别为 2.1~2.4 Ga 左右的大氧化事件(Great Oxidation Event;GOE)和 0.75~0.58 Ga 左右的新元古代氧化事件(Neoproterozoic Oxygenation Event; NOE)(Kump, 2008; Lyons et al., 2014)。在大气圈增氧过程中,新元古代成冰纪地球上发生了几次全球性的冰川事件,冰雪甚至

覆盖率中低纬度和磁道地区(即“雪球地球”; Hoffman et al., 1998)。其中可进行全球对比的两次冰期为 Sturtian 冰期和 Marinoan 冰期,分别对应华南地区的江口冰期和南沱冰期(赵彦彦和郑永飞, 2011; 张启锐和兰中伍, 2016; 旷红伟等, 2019)。在两次冰期之间的间冰期期间,华南地区南华盆地沉积了深水相大塘坡组(或相当层位),主要分布在黔—湘—渝等地区。

南华纪时期, Rodinia 超大陆的裂解作用形成了南华裂谷盆地,其为大塘坡组锰矿的堆积提供可容空间(王剑等, 2001; 杜远生等, 2018)。另一方面,断陷活动形成的断裂系统可为深部热液提供通道,这些热液作为沉积水体中锰、铁等物质的重要来源,为华南地区大塘坡锰矿提供主要的成矿物质来源(张飞飞等, 2013; Yu Wenchao et al., 2016; Wang Ping et al., 2019)。此外,大陆风化作用强度的指标(如 *CIA*、锂同位素、锇同位素组成等)显示,在 Sturtian 冰期结束前夕,气候表现为从冰期寒冷干燥逐渐转为温暖潮湿,逐渐增强的大陆风化作用也为大塘坡锰矿提供了大量的成矿物质(李明龙等, 2019; Wang Ping et al., 2020; Wei Guangyi et al., 2020)。Sturtian 冰期结束后,随着冰盖的消融及大气氧气含量的增加,南华盆地表层海水逐渐被氧化,但深部水体仍保持还原的特性(Li Chao et al., 2012; Wei Wei et al., 2016; Cheng Meng et al., 2018; Wang Ping et al., 2019)。在这种氧化还原分层的水体中,Mn^{2+} 离子首先在还原性缺氧水体中逐渐富集;上升流携带的 Mn^{2+} 离子运移至氧化还原界面之上被氧化形成锰氧化物(或氢氧化物)发生沉淀;随着上覆沉积物的堆积,沉积物—水界面之下逐渐演变为一个还原的微环境,锰氧化物(或氢氧化物)被微生物还原成 Mn^{2+} 离子,其与孔隙水中的碳酸根(CO_3^{2-})离子结合形成碳酸锰(即菱锰矿)发生沉淀(Roy, 2006; Maynard, 2014)。此外,近期研究表明,冰川消融形成的间歇性氧化底流可能会造成盆地深部水体发生部分间歇性氧化(Yu Wenchao et al., 2016; Wang Ping et al., 2020)。近期研究显示,在沉积期 Mn^{2+} 氧化固定过程和早期成岩阶段 MnO_2 的再还原与碳酸锰沉淀过程中,微生物可能也起着非常重要的作用(Fan Delian et al., 1999; Yu Wenchao et al., 2019)。

5 结论

(1)南华盆地 Sturtian 冰期的启动和结束与全球其他地区基本一致,分别发生在~717 Ma 和~660 Ma 之前,持续时间约为 57 Ma;且南华盆地南华系大塘坡锰矿大约形成于~660 Ma 之前。

(2)在 Rodinia 超大陆裂解作用的影响下,南华裂谷盆地内部发育一系列由同沉积断层控制的地垒—地堑次级盆地,为锰质的沉淀提供了可容空间;同时,深部热液为大塘坡锰矿的形成提供了大量的成矿物质,并对大塘坡锰矿的发育具有明显的控制作用。

(3)南华盆地 Sturtian 冰期晚期至间冰期大塘坡期早期的气候主要为寒冷干燥,随后转为温暖湿润并很快变为寒冷干燥。至大塘坡期中晚期,气候逐渐由寒冷干燥恢复至温暖湿润,并一直保持至大塘坡期晚期。

(4)Sturtian 冰期结束后,南华盆地表层海水逐渐氧化,深部沉积水体出现局部间歇式氧化环境,热液和陆源输入的 Mn^{2+} 被氧化为 MnO_2 发生沉淀,并在早期成岩阶段在微生物的作用下最终形成菱锰矿。

致谢:感谢评审专家和责任编辑对本文修改提出的宝贵建议。

参 考 文 献 / References

(The literature whose publishing year followed by a “**&**” is in Chinese with English abstract; The literature whose publishing year followed by a “**#**” is in Chinese without English abstract)

蔡娟娟, 崔晓庄, 兰中伍, 王剑, 江卓斐, 邓奇, 卓皆文, 陈风霖, 江新胜. 2018. 华南扬子陆块成冰纪冰川作用的启动时限及其全球对比. 古地理学报, 20(1): 65~86.

董志国, 张连昌, 王长乐, 张帮禄, 彭自栋, 朱明田, 冯京, 谢月桥. 2020. 沉积碳酸锰矿床研究进展及有待深入探讨的若干问题. 矿床地质, 39(2): 237~255.

杜远生, 周琦, 余文超, 王萍, 袁良军, 齐靓, 郭华, 徐源. 2015. Rodinia 超大陆裂解、Sturtian 冰期事件和扬子地块东南缘大规模锰成矿作用. 地质科技情报, 34(6): 1~7.

杜远生, 周琦, 余文超, 张亚冠, 王萍, 覃永军, 庞大卫. 2018. 贵州南华纪—震旦纪沉积大地构造及其对沉积矿产的控制作用. 贵州地质, 35(4): 282~290.

冯连君, 储雪蕾, 张同钢, 黄晶. 2006. 莲沱砂岩——南华大冰期前气候转冷的沉积记录. 岩石学报, 22(9): 2387~2393.

付勇, 徐志刚, 裴浩翔, 江冉. 2014. 中国锰矿成矿规律初探. 地质学报, 88(12): 2192~2207.

高林志, 陆济璞, 丁孝忠, 王汉荣, 刘燕学, 李江. 2013. 桂北地区新元古代地层凝灰岩锆石 U-Pb 年龄及地质意义. 中国地质, 40(5): 1443~1452.

苟龙飞, 金章东, 贺茂勇. 2017. 锂同位素示踪大陆风化: 进展与挑战. 地球环境学报, 8(2): 89~102.

何志威, 杨瑞东, 高军波, 程伟, 刘帅, 张峰玮. 2014. 贵州松桃道坨锰矿含锰岩系地球化学特征和沉积环境分析. 地质论评, 60(5): 1061~1075.

旷红伟, 柳永清, 耿元生, 白华青, 彭楠, 范正秀, 宋换新, 夏晓旭, 王玉冲, 陈骁帅. 2019. 中国中新元古代重要沉积地质事件及其意义. 古地理学报, 21(1): 1~30.

李超, 屈文俊, 王登红, 周利敏, 杜安道, 付勇, 裴浩翔. 2014. Re-Os 同位素在沉积地层精确定年及古环境反演中的应用进展. 地球学报, 35(4): 405~414.

李明龙, 陈林, 田景春, 郑德顺, 许克元, 方喜林, 曹文胜, 赵军, 冉中夏. 2019. 鄂西走马地区南华纪古城期—南沱早期古气候和古氧相演化: 来自细碎屑岩元素地球化学的证据. 地质学报, 93(9): 2158~2170.

李明龙, 杨波涌, 郑德顺, 陈林, 田景春. 2021. 鄂西走马地区南华纪大塘坡间冰期古气候研究. 地质论评, 67(1): 39~55.

凌云, 马志鑫, 杨弘忠, 刘振, 刘伟, 张礼敏, 李波. 2016. 重庆秀山南华纪大塘坡期沉积相分析与锰矿成矿. 地质科技情报, 35(6): 150~156.

裴浩翔, 付勇, 李超, 李延河, 安正泽. 2017. 贵州道坨锰矿成矿时代及环境的 Re-Os 同位素证据. 科学通报, 62(Z2): 3346~3355.

裴浩翔, 李延河, 付勇, 占朋才. 2020. 贵州铜仁高地"大塘坡式"锰矿的成矿机制——硫、碳同位素制约. 地球学报, 41(5): 651~662.

齐靓, 余文超, 杜远生, 周琦, 郭华, 王佳武, 王萍, 徐源. 2015. 黔东南华纪铁丝坳期—大塘坡期古气候的演变: 来自 *CIA* 的证据. 地质科技情报, 34(6): 47~57.

覃永军, 杜远生, 牟军, 卢定彪, 龙建喜, 王安华, 张厚松 ,曾昌兴. 2015. 黔东南地区新元古代下江群的地层年代及其地质意义. 地球科学(中国地质大学学报), 40(7): 1107~1131.

史富强, 朱祥坤, 闫斌, 刘燕群, 张飞飞, 赵妮娜, 褚明恺. 2016. 湖南湘潭锰矿的地球化学特征及成矿机制. 岩石矿物学杂志, 35(3): 443~456.

孙海清, 黄建中, 江新胜, 罗来, 马慧英, 伍皓. 2013. 扬子东南缘"南华纪"盆地演化——来自新元古代花岗岩的年龄约束. 中国地质, 40(6): 1725~1735.

汪正江, 王剑, 江新胜, 孙海清, 高天山, 陈建书, 邱艳生, 杜秋定, 邓奇, 杨菲. 2015. 华南扬子地区新元古代地层划分对比研究新进展. 地质论评, 61(1): 1~22.

王富良, 付勇, 江冉, 周文喜, 葛枝华, 魏帅超, 梁厚鹏, 张鹏. 2016. Re-Os 同位素在晚新元古代至早寒武世测年及古环境演绎中的应用进展. 岩矿测试, 35(5): 530~541.

王剑, 刘宝珺, 潘桂棠. 2001. 华南新元古代裂谷盆地演化——Rodinia 超大陆解体的前奏. 矿物岩石, 21(3): 135~145.

王霄, 李艳, 黎晏彰, 刘雨薇, 段鉴书, 丁竑瑞, 王长秋, 鲁安怀. 2018&. 浅海 Mg^{2+} 和 SO_4^{2-} 对微生物诱导形成锰碳酸盐的影响. 地球科学, 43(S1): 145~156.

王孝磊, 周金城, 邱检生, 高剑峰. 2004. 湘东北新元古代强过铝花岗岩的成因: 年代学和地球化学证据. 地质论评, 50(1): 65~76.

王自强, 高林志, 丁孝忠, 黄志忠. 2012. "江南造山带"变质基底形成的构造环境及演化特征. 地质论评, 58(3): 401~413.

尹崇玉, 王砚耕, 唐烽, 万渝生, 王自强, 高林志, 邢裕盛, 刘鹏举. 2006. 贵州松桃南华系大塘坡组凝灰岩锆石 SHRIMP Ⅱ U-Pb 年龄. 地质学报, 80(2): 273~278.

余文超, 杜远生, 周琦, 彭头平, 王萍, 袁良军, 徐源, 潘文, 谢小峰, 齐靓. 2016a. 黔东松桃南华系大塘坡组锰矿层物源: 来自 Sr 同位素的证据. 地球科学, 41(7): 1110~1120.

余文超, 杜远生, 周琦, 王萍, 齐靓, 徐源, 靳松, 潘文, 袁良军, 谢小峰, 杨炳南. 2020. 华南成冰纪"大塘坡式"锰矿沉积成矿作用与重大地质事件的耦合关系. 古地理学报, 22(5): 855~871.

余文超, 杜远生, 周琦, 王萍, 袁良军, 徐源, 潘文, 谢小峰, 齐靓, 焦良轩. 2016b. 黔东松桃地区大塘坡组 LA-ICP-MS 锆石 U-Pb 年龄及其地质意义. 地质论评, 62(3): 539~549.

张飞飞, 朱祥坤, 高兆富, 程龙, 彭乾云, 杨德智. 2013. 黔东北西溪堡锰矿的沉淀形式与含锰层位中黄铁矿异常高 $\delta^{34}S$ 值的成因. 地质论评, 59(2): 274~286.

张启锐, 兰中伍. 2016. 南华系、莲沱组年龄问题的讨论. 地层学杂志, 40(3): 297~301.

张予杰, 安显银, 刘石磊, 高永娟, 郑杰, 桑永恒. 2020. 黔东北地区大塘坡组早期含锰沉积充填、岩相古地理与锰矿的关系. 中国地质, 47(3): 607~626.

赵军红, 王伟, 刘航. 2015. 扬子东南缘新元古代地质演化. 矿物岩石地球化学通报, 34(2): 227~233.

赵彦彦, 郑永飞. 2011. 全球新元古代冰期的记录和时限. 岩石学报, 27(2): 545~565.

赵志强, 凌云, 李核良, 蒋凯, 李杰, 蔡柯柯, 廖洪. 2019. 重庆秀山小茶园大塘坡组含锰岩系地球化学特征及地质意义. 矿物岩石地球化学通报, 38(2): 330~341.

周琦, 杜远生, 覃英. 2013. 古天然气渗漏沉积型锰矿床成矿系统与成矿模式——以黔湘渝毗邻区南华纪"大塘坡式"锰矿为例. 矿床地质, 32(3): 457~466.

周琦, 杜远生, 袁良军, 张遂, 余文超, 杨胜堂, 刘雨. 2016. 黔湘渝毗邻区南华纪武陵裂谷盆地结构及其对锰矿的控制作用. 地球科学, 41(2): 177~188.

朱祥坤, 彭乾云, 张仁彪, 安正泽, 张飞飞, 闫斌, 李津, 高兆富, 覃英, 潘文. 2013. 贵州省松桃县道坨超大型锰矿床地质地球化学特征. 地质学报, 87(9): 1335~1348.

邹光均, 黄建中, 凌跃新, 谭仕敏, 曹创华, 黄革非, 文春华. 2020. 湘黔渝毗邻区南华纪岩相古地理及沉积盆地演化. 地球学报, 41(2): 207~218.

Allen P A, Bowring S, Leather J, Brasier M, Cozzi A, Grotzinger J P, McCarron G, Amthor J J. 2002. Chronology of Neoproterozoic gla*CIA*tions: New insights from Oman. International Sedimentological Congress, 16th, Johannesburg, South Africa, July 8~12, Abstract Volume: 7~8.

Anbar A D, Duan Y, Lyons T W, Arnold G L, Kendall B, Creaser R A, Kaufman A J, Gordon G W, Scott C, Garvin J, Buick R. 2007. A whiff of oxygen before the great oxidation event? Science, 317(5846): 1903~1906.

Bahlburg H, Dobrzinski N. 2011. A review of the Chemical Index of Alteration (*CIA*) and its application to the study of Neoproterozoic glacial deposits and climate transitions, In: Arnaud E, Halverson G P, Shield-Zhou G, Geological T (Eds.), Record of Neoproterozoic Glaciations. Geological Society, London, Memoirs, 36: 81~92.

Bowring S A, Grotzinger J P, Condon D J, Ramezani J, Newall M J, Allen P A. 2007. Geochronologic constraints on the chronostratigraphic framework of the Neoproterozoic Huqf Supergroup, Sultanate of Oman. American Journal of Science, 307(10): 1097~1145.

Cai Juanjuan, Cui Xiaozhuang, Lan Zhongwu, Wang Jian, Jiang Zhuofei, Deng Qi, Zhuo Jiewen, Chen Fenglin, Jiang Xinsheng. 2018&. Onset time and global correlation of the Cryogenian glaciations in Yangtze Block, South China. Journal of Palaeogeography (Chinese Edition), 20(1): 65~86.

Canfield D E. 2005. The early history of atmospheric oxygen: Homage to Robert M. Garrels. Annual Review of Earth and Planetary Sciences, 33(1): 1~36.

Chen Xi, Li Da, Ling Hongfei, Jiang Shaoyong. 2008. Carbon and sulfur isotopic compositions of basal Datangpo Formation, northeastern Guizhou, South China: Implications for depositional environment. Progress in Natural Science, 18(4): 421~429.

Cheng Meng, Li Chao, Chen Xi, Zhou Lian, Algeo T J, Ling Hongfei, Feng Lianjun, Jin Chengsheng. 2018. Delayed Neoproterozoic oceanic oxygenation: Evidence from Mo isotopes of the Cryogenian Datangpo Formation. Precambrian Research, 319: 187~197.

Cohen A S. 2004. The rhenium-osmium isotope system: applications to geochronological and palaeoenvironmental problems. Journal of the Geological Society, 161(4): 729~734.

Cohen A S, Coe A L, Bartlett J M, Hawkesworth C J. 1999. Precise Re-Os ages of organic-rich mudrocks and the Os isotope composition of Jurassic seawater. Earth and Planetary Science Letters, 167(3~4): 159~173.

Cole D B, Mills D B, Erwin D H, Sperling E A, Porter S M, Reinhard C T, Planavsky N J. 2020. On the co-evolution of surface oxygen levels and animals. Geobiology, 18(3): 260~281.

Cox G M, Halverson G P, Minarik W G, Le Heron D P, Macdonald F A, Bellefroid E J, Strauss J V. 2013. Neoproterozoic iron formation: An evaluation of its temporal, environmental and tectonic significance. Chemical Geology, 362: 232~249.

Cox G M, Isakson V, Hoffman P F, Gernon T M, Schmitz M D, Shahin S, Collins A S, Preiss W, Blades M L, Mitchell R N, Nordsvan A. 2018. South Australian U-Pb zircon (CA-ID-TIMS) age supports globally synchronous Sturtian deglaciation. Precambrian Research, 315: 257~263.

Creaser R A, Sannigrahi P, Chacko T, Selby D. 2002. Further evaluation of the Re-Os geochronometer in organic-rich sedimentary rocks: A test of hydrocarbon maturation effects in the Exshaw Formation, Western Canada Sedimentary Basin. Geochimica et Cosmochimica Acta, 66(1): 3441~3452.

Dong Zhiguo, Zhang Llianchang, Wang Changle, Zhang Banglu, Peng Zidong, Zhu Mingtian, Feng Jing, Xie Yueqiao. 2020&. Progress and problems in understanding sedimentary manganese carbonate metallogenesis. Mineral Deposits, 39(2): 237~255.

Du Yuansheng, Zhou Qi, Yu Wenchao, Wang Ping, Yuan Liangjun, Qi Liang, Guo Hua, Xu Yuan. 2015&. Linking the Cryogenian manganese metallogenic process in Southeast margin of Yangtze Block to break-up of Rodinia Supercontinent and Sturtian glaciation. Geological Science and Technology Information, 34(6): 1~7.

Du Yuansheng, Zhou Qi, Yu Wenchao, Zhang Yaguan, Wang Ping, Qin Yongjun, Pang Dawei. 2018&. Sedimentary geotectonics and its control function of sedimentary mineral in Nanhua Period—Sinian Period in Guizhou. Guizhou Geology, 35(4): 282~290.

Esser B K, Turekian K K. 1993. The osmium isotopic composition of the continental crust. Geochimica et Cosmochimica Acta, 57(13): 3093~3104.

Evans D V D, Lund K, Aleinikoff J N, Fanning C M. 1997. SHRIMP U-Pb age of late Proterozoic volcanism in central Idaho. In Geological Society of America Abstracts with Programs, 29(6): A196.

Fan Delian, Ye Jie, Yin Leiming, Zhang Rufan. 1999. Microbial processes in the formation of the Sinian Gaoyan manganese carbonate ore, Sichuan Province, China. Ore Geology Reviews, 15(1~3): 79~93.

Fan Haifeng, Wen Hanjie, Han Tao, Zhu Xiangkun, Feng Lianjun, Chang Huajin. 2018. Oceanic redox condition during the late Ediacaran (551 ~ 541 Ma), South China. Geochimica et Cosmochimica Acta, 238: 343~356.

Fanning C M, Link P. 2008. Age constraints for the Sturtian glaciation: data from the Adelaide Geosyncline, South Australia and Pocatello Formation, Idaho, USA, In: Selwyn Symposium. The Geological Society of Australia, vol. Abstract, 57~62.

Fanning C M, Link P K. 2004. U-Pb SHRIMP ages of Neoproterozoic (Sturtian) glaciogenic Pocatello Formation, southeastern Idaho. Geology, 32(10): 881~884.

Fanning C M, Link P K. 2006. Constraints on the timing of the Sturtian glaciation from southern Australia: i. e. for the true Sturtian GSA. Geological Society of America Abstracts with Programs, 38(7): 115.

Feng Lianjun, Chu Xuelei, Zhang Tonggang, Huang Jing. 2006&. Liantuo sandstones: sedimentary records under cold climate before the Nanhua big glaciations. Acta Petrologica Sinica, 22(9): 2387~2393.

Ferri F, Rees C J, Nelson J L, Legun A S. 1999. Geology and mineral deposits of the northern Kechika Trough between Gataga River and the 60th paralle. British Columbia Ministry of Energy and Mines, Bulletin, 107: 1~122.

Finlay A J, Selby D, Gröcke D R. 2010. Tracking the Hirnantian glaciation using Os isotopes. Earth and Planetary Science Letters, 293(3~4): 339~348.

Force E R, Cannon W F. 1988. Depositional model for shallow-marine manganese deposits around black shale basins. Economic Geology, 83(1): 93~117.

Fu Yong, Dong Lin, Li Chao, Qu Wenjun, Pei Haoxiang, Qiao Wenlang, Shen Bing. 2016. New Re-Os isotopic constrains on the formation of the metalliferous deposits of the Lower Cambrian Niutitang formation. Journal of Earth Science, 27(2): 271~281.

Fu Yong, Xu Zhigang, Pei Haoxiang, Jiang Ran. 2014&. Study on metallogenic regularity of manganese ore deposits in China. Acta Geologica Sinica, 88(12): 2192~2207.

Gao Linzhi, Lu Jipu, Ding Xiaozhong, Wang Hanrong, Liu Yanxue, Li Jiang. 2013&. Zircon U-Pb dating of Neoproterozoic tuff in South Guangxi and its implications for stratigraphic correlation. Geology in China, 40(5): 1443~1452.

Gibson T M, Wörndle S, Crockford P W, Bui T H, Creaser R A, Halverson G P. 2019. Radiogenic isotope chemostratigraphy reveals marine and nonmarine depositional environments in the late Mesoproterozoic Borden Basin, Arctic Canada. GSA Bulletin, 131(11~12): 1965~1978.

Gou Longfei, Jin Zhangdong, He Maoyong. 2017&. Using lithium isotopes traces continental weathering: Progresses and challenges. Journal of Earth Environment, 8(2): 89~102.

Hannah J L, Bekker A, Stein H J, Markey R J, Holland H D. 2004. Primitive Os and 2316 Ma age for marine shale: implications for Paleoproterozoic glacial events and the rise of atmospheric oxygen. Earth and Planetary Science Letters, 225(1~2): 43~52.

He Zhiwei, Yang Ruidong, Gao Junbo, Cheng Wei, Liu Shuai, Zhang Fengwei. 2014&. Geochemical characteristics and sedimentary environment of manganese-bearing rock series of Daotuo, manganese deposit, Songtao County of Guizhou Province. Geological Review, 60(5): 1061~1075.

Hoffman P F. 1991. Did the breakout of Laurentia turn Gondwanaland inside-out? Science, 252(5011): 1409~1412.

Hoffman P F, Abbot D S, Ashkenazy Y, Benn D I, Brocks J J, Cohen P

A, Cox G M, Creveling J R, Donnadieu Y, Erwin D H, Fairchild I J, Ferreira D, Goodman J C, Halverson G P, Jansen M F, Le Hir G, Love G D, Macdonald F A, Maloof A C, Partin C A, Ramstein G, Rose B E J, Rose C V, Sadler P M, Tziperman E, Voigt A, Warren S G. 2017. Snowball Earth climate dynamics and Cryogenian geology—geobiology. Science Advances, 3(11): e1600983. doi: 10.1126/sciadv.1600983.

Hoffman P F, Kaufman A J, Halverson G P, Schrag D P. 1998. A Neoproterozoic snowball earth. Science, 281(5381): 1342~1346.

Hoffman P F, Li Z X. 2009. A palaeogeographic context for Neoproterozoic glaciation. Palaeogeography, Palaeoclimatology, Palaeoecology, 277(3~4): 158~172.

Hoffman P F, Schrag D P. 2002. The snowball Earth hypothesis: testing the limits of global change. Terra Nova, 14(3): 129~155.

Huang Kangjun, Teng Fangzhen, Shen Bing, Xiao Shuhai, Lang Xianguo, Ma Haoran, Fu Yong, Peng Yongbo. 2016. Episode of intense chemical weathering during the termination of the 635 Ma Marinoan glaciation. Proceedings of the National Academy of Sciences, 113(52): 14904~14909.

Huang Taiyu, Chen Daizhao, Fu Yong, Yeasmin Rumana, Guo Chuan. 2019. Development and evolution of a euxinic wedge on the ferruginous outer shelf of the early Cambrian Yangtze sea. Chemical Geology, 524: 259~271.

Huckriede H, Meischner D. 1996. Origin and environment of manganese-rich sediments within black-shale basins. Geochimica et Cosmochimica Acta, 60(8): 1399~1413.

Jiang Zhuofei, Cui Xiaozhuang, Jiang Xinsheng, Wang Jian, Zhuo Jiewen, Xiong Guoqing, Lu Junze, Wu Hao, Wei Yanan. 2016. New zircon U-Pb ages of the pre-Sturtian rift successions from the western Yangtze Block, South China and their geological significance. International Geology Review, 58(9): 1064~1075.

Johnsson M J, Stallard R F, Lundberg N. 1991. Controls on the composition of fluvial sands from a tropical weathering environment: Sands of the Orinoco River drainage basin, Venezuela and Colombia. Geological Society of America Bulletin, 103(12): 1622~1647.

Kendall B, Creaser R A, Selby D. 2006. Re-Os geochronology of postglacial black shales in Australia: Constraints on the timing of "Sturtian" glaciation. Geology, 34(9): 729~732.

Kendall B, Creaser R A, Selby D. 2009. ^{187}Re-^{187}Os geochronology of Precambrian organic-rich sedimentary rocks. Geological Society, London, Special Publications, 326(1): 85~107.

Kendall B S, Creaser R A, Ross G M, Selby D. 2004. Constraints on the timing of Marinoan "Snowball Earth" glaciation by ^{187}Re-^{187}Os dating of a Neoproterozoic, post-glacial black shale in Western Canada. Earth and Planetary Science Letters, 222(3~4): 729~740.

Krauskopf K B. 1957. Separation of manganese from iron in sedimentary processes. Geochimica et Cosmochimica Acta, 12(1~2): 61~84.

Kuang Hongwei, Liu Yongqing, Geng Yuansheng, Bai Huaqing, Peng Nan, Fan Zhengxiu, Song Huanxin, Xia Xiaoxu, Wang Yuchong, Chen Xiaoshuai. 2019&. Important sedimentary geological events of the Meso—Neoproterozoic and their significance. Journal of Palaeogeography (Chinese Edition), 21(1): 1~30.

Kump L R. 2008. The rise of atmospheric oxygen. Nature, 451(7176): 277~278.

Lan Zhongwu, Li Xianhua, Zhu Maoyan, Chen Zhongqiang, Zhang Qirui, Li Qiuli, Lu Dingbiao, Liu Yu, Tang Guoqiang. 2014. A rapid and synchronous initiation of the wide spread Cryogenian glaciations. Precambrian Research, 255: 401~411.

Lan Zhongwu, Li Xianhua, Zhu Maoyan, Zhang Qirui, Li Qiuli. 2015. Revisiting the Liantuo Formation in Yangtze Block, South China: SIMS U-Pb zircon age constraints and regional and global significance. Precambrian Research, 263: 123~141.

Lan Zhongwu, Huyskens M H, Lu Kai, Li Xianhua, Zhang Gangyang, Lu Dingbiao, Yin Qingzhu. 2020. Toward refining the onset age of Sturtian glaciation in South China. Precambrian Research, 338: 105555. doi: 10.1016/j.precamres.2019.105555.

Levasseur S, Birck J L, Allègre C J. 1998. Direct measurement of femtomoles of osmium and the ^{187}Os/^{186}Os ratio in seawater. Science, 282(5387): 272~274.

Li Chao, Love G D, Lyons T W, Scott C T, Feng Lianjun, Huang Jing, Chang Huajin, Zhang Qirui, Chu Xuelei. 2012. Evidence for a redox stratified Cryogenian marine basin, Datangpo Formation, South China. Earth and Planetary Science Letters, 331~332: 246~256.

Li Chao, Qu Wenjun, Wang Denghong, Zhou Limin, Du Andao, Fu Yong, Pei Haoxiang. 2014&. The progress of applying Re-Os isotope to dating of organic-rich sedimentary rocks and reconstruction of paleoenvironment. Acta Geoscientica Sinica, 35(4): 405~414.

Li Chao, Zhang Zihu, Jin Chengsheng, Cheng Meng, Wang Haiyang, Huang Junhua, Algeo T J. 2020. Spatiotemporal evolution and causes of marine euxinia in the early Cambrian Nanhua Basin (South China). Palaeogeography, Palaeoclimatology, Palaeoecology, 546: 109676. doi: 10.1016/j.palaeo.2020.109676.

Li Jian, Hao Cuiguo, Wang Zhihong, Dong Lin, Wang Yiwu, Huang Kangjun, Lang Xianguo, Huang Tianzheng, Yuan Honglin, Zhou Chuanming, Shen Bing. 2020. Continental weathering intensity during the termination of the Marinoan Snowball Earth: Mg isotope evidence from the basal Doushantuo cap carbonate in South China. Palaeogeography, Palaeoclimatology, Palaeoecology, 552: 109774. doi: 10.1016/j.palaeo.2020.109774.

Li Qiwei, Zhao Junhong. 2020. Amalgamation between the Yangtze and Cathaysia blocks in South China: Evidence from the ophiolite geochemistry. Precambrian Research, 350: 105893. doi: 10.1016/j.precamres.2020.105893.

Li Z X, Bogdanova S V, Collins A S, Davidson A, De Waele B, Ernst R E, Fitzsimons I C W, Fuck R A, Gladkochub D P, Jacobs J, Karlstrom K E, Lu S, Natapov L M, Pease V, Pisarevsky S A, Thrane K, Vernikovsky V. 2008. Assembly, configuration, and break-up history of Rodinia: A synthesis. Precambrian Research, 160(1~2): 179~210.

Li Minglong, Chen Lin, Tian Jingchun, Zheng Deshu, Xu Keyuan, Fang Xilin, Cao Wensheng, Zhao Jun, Ran Zhongxia. 2019&. Paleoclimate and paleo- oxygen evolution during the Gucheng Period—early Nantuo Period of Nanhua System in the Zouma area, West Hubei: evidence from elemental geochemistry of fine clastic rocks. Acta Geologica Sinica, 93(9): 2158~2170.

Li Minglong, Yang Boyong, Zheng Deshun, Chen Lin, Tian Jingchun. 2021&. Study on the paleoclimate during the Datangpo interglacial stage of the Nanhua Period in the Zouma area, western Hubei Province, Geological Review, 67(1): 39~55.

Ling Yun,, Ma Zhixin, Yang Hongzhong, Liu Zhen, Liu Wei, Zhang Limin, Li Bo. 2016&. Sedimentary facies analysis of Datangpo Formation and manganese minerallization at Xiushan, Chongqing. Geological Science and Technology Information, 35(6): 150~156.

Lu Zunli, Jenkyns H C, Rickaby R E M. 2010. Iodine to calcium ratios in marine carbonate as a paleo-redox proxy during oceanic anoxic events. Geology, 38(12): 1107~1110.

Lund K, Aleinikoff J N, Evans K V, Fanning C M. 2003. SHRIMP U-Pb geochronology of Neoproterozoic Windermere Supergroup, central Idaho: Implications for rifting of western Laurentia and synchroneity of Sturtian glacial deposits. Geological Society of America Bulletin, 115(3): 349~372.

Lyons T W, Reinhard C T, Planavsky N J. 2014. The rise of oxygen in Earth's early ocean and atmosphere. Nature, 506(7488): 307~315.

Ma Zhixin, Liu Xiting, Yu Wenchao, Du Yuansheng, Du Qiuding. 2019. Redox conditions and manganese metallogenesis in the Cryogenian Nanhua Basin: Insight from the basal Datangpo Formation of South China. Palaeogeography, Palaeoclimatology, Palaeoecology, 529: 39~52.

Macdonald F A, Schmitz M D, Crowley J L, Roots C F, Jones D S, Maloof A C, Strauss J V, Cohen P A, Johnston D T, Schrag D P. 2010. Calibrating the Cryogenian. Science, 327(5970): 1241~1243.

Macdonald F A, Schmitz M D, Strauss J V, Halverson G P, Gibson T M, Eyster A, Cox G, Mamrol P, Crowley J L. 2018. Cryogenian of Yukon. Precambrian Research, 319: 114~143.

Maynard J B. 2010. The chemistry of manganese ores through time: A signal of increasing diversity of Earth-surface environments. Economic Geology, 105(3): 535~552.

Maynard J B. 2014. Manganiferous sediments, rocks, and ores, In: Holland H D, Turekian K K (Eds.), Treatise on geochemistry (Second Edition). Oxford: Elsevier: 327~349.

McLennan S M. 1993. Weathering and global denudation. The Journal of Geology, 101(2): 295~303.

Meisel T, Walker R J, Irving A J, Lorand J P. 2001. Osmium isotopic compositions of mantle xenoliths: a global perspective. Geochimica et Cosmochimica Acta, 65(8): 1311~1323.

Mucci A. 2004. The behavior of mixed Ca—Mn carbonates in water and seawater: controls of manganese concentrations in marine porewaters. Aquatic Geochemistry, 10(1): 139~169.

Nesbitt H W, Young G M. 1982. Early Proterozoic climates and plate motions inferred from major element chemistry of lutites. Nature, 299(5885): 715~717.

Nesbitt H W, Young G M. 1989. Formation and diagenesis of weathering profiles. The Journal of Geology, 97(2): 129~147.

Pei Haoxiang, Fu Yong, Li Chao, Li Yanhe, An Zhengze. 2017&. Mineralization age and metallogenic environment of Daotuo manganese deposits in Guizhou: Evidence from Re-Os isotopes. Chinese Science Bulletin, 62(28~29): 3346~3355.

Pei Haoxiang, Li Yanhe, Fu Yong, Zhan Pengcai. 2020&. Metallogenic mechanism of "Datangpo Type" manganese deposits in Gaodi, Guizhou Province: Constrains from sulfur and carbon isotopes. Acta Geoscientica Sinica, 41(5): 651~662.

Peucker-Ehrenbrink B, Ravizza G. 2000. The marine osmium isotope record. Terra Nova, 12(5): 205~219.

Pufahl P K, Anderson S L, Hiatt E E. 2014. Dynamic sedimentation of Paleoproterozoic continental margin iron formation, Labrador Trough, Canada: Paleoenvironments and sequence stratigraphy. Sedimentary Geology, 309: 48~65.

Qin Yongjun, Du Yuansheng, Mou Jun, Lu Dingbiao, Long Jianxi, Wang Anhua, Zhang Housong, Zeng Changxing. 2015&. Geochronology of Neoproterozoic Xiajiang Group in Southeast Guizhou, South China, and its geological implication. Earth Science——Journal of China University of Geosciences, 40(7): 1107~1131.

Rasmussen B. 2005. Radiometric dating of sedimentary rocks: the application of diagenetic xenotime geochronology. Earth-Science Reviews, 68(3~4): 197~243.

Ravizza G, Turekian K K. 1989. Application of the ^{187}Re-^{187}Os system to black shale geochronometry. Geochimica et Cosmochimica Acta, 53(12): 3257~3262.

Rooney A D, Chew D M, Selby D. 2011. Re-Os geochronology of the Neoproterozoic—Cambrian Dalradian Supergroup of Scotland and Ireland: Implications for Neoproterozoic stratigraphy, glaciations and Re-Os systematics. Precambrian Research, 185(3~4): 202~214.

Rooney A D, Macdonald F A, Strauss J V, Dudas F O, Hallmann C, Selby D. 2014. Re-Os geochronology and coupled Os-Sr isotope constraints on the Sturtian snowball Earth. Proceedings of the National Academy of Sciences, 111(1): 51~56.

Rooney A D, Selby D, Houzay J-P, Renne P R. 2010. Re-Os geochronology of a Mesoproterozoic sedimentary succession, Taoudeni basin, Mauritania: Implications for basin-wide correlations and Re-Os organic-rich sediments systematics. Earth and Planetary Science Letters, 289(3~4): 486~496.

Rooney A D, Strauss J V, Brandon A D, Macdonald F A. 2015. A Cryogenian chronology: Two long-lasting synchronous Neoproterozoic glaciations. Geology, 43(5): 459~462.

Rooney A D, Yang C, Condon D J, Zhu M, Macdonald F A. 2020. U-Pb and Re-Os geochronology tracks stratigraphic condensation in the Sturtian snowball Earth aftermath. Geology, 48(6): 625~629.

Rotich E K, Handler M R, Naeher S, Selby D, Hollis C J, Sykes R. 2020. Re-Os geochronology and isotope systematics, and organic and sulfur geochemistry of the middle—late Paleocene Waipawa Formation, New Zealand: Insights into early Paleogene seawater Os isotope composition. Chemical Geology, 536: 119473. doi: 10.1016/j. chemgeo. 2020. 119473.

Roy S. 2006. Sedimentary manganese metallogenesis in response to the evolution of the Earth system. Earth-Science Reviews, 77(4): 273~305.

Sahoo S K, Planavsky N J, Jiang G, Kendall B, Owens J D, Wang X, Shi X, Anbar A D, Lyons T W. 2016. Oceanic oxygenation events in the anoxic Ediacaran ocean. Geobiology, 14(5): 457~468.

Schoenborn W A, Fedo C M. 2011. Provenance and paleoweathering reconstruction of the Neoproterozoic Johnnie Formation, southeastern California. Chemical Geology, 285(1~4): 231~255.

Semikhatov M A. 1991. General problems of Proterozoic stratigraphy in the USSR Soviet Science Review G (Geology), 1: 1~192.

Sheldon N D, Tabor N J. 2009. Quantitative paleoenvironmental and paleoclimatic reconstruction using paleosols. Earth-Science Reviews, 95(1~2): 1~52.

Shi Fuqiang, Zhu Xiangkun, Yan Bin, Liu Yanqun, Zhang Feifei, Zhao Nina, Chu Mingkai. 2016&. Geochemical charateristics and metallogenic mechanism of the Xiangtan manganese ore deposits in Hunan Province. Acta Petrologica et Mineralogica, 35(3): 443~456.

Shirey S B, Walker R J. 1998. The Re-Os isotope system in cosmochemistry and high-temperature geochemistry. Annual Review of Earth and Planetary Sciences, 26(1): 423~500.

Sun Haiqing, Huang Jianzhong, Jiang Xinsheng, Luo Lai, Ma Huiying,

Wu Hao. 2013&. The evolution of "Nanhuaian" rift basin based on the southeastern margin of Yangtze platform: Age constraints from the Neoproterozoic granites. Geology in China, 40(6): 1725~1735.

Song Gaoyuan, Wang Xinqiang, Shi Xiaoying, Jiang Ganqing. 2017. New U-Pb age constraints on the upper Banxi Group and synchrony of the Sturtian glaciation in South China. Geoscience Frontiers, 8(5): 1161~1173.

Tan Zhaozhao, Jia Wanglu, Li Jie, Yin Lu, Wang Susu, Wu Jinxiang, Song Jianzhong, Peng Ping'an. 2021. Geochemistry and molybdenum isotopes of the basal Datangpo Formation: Implications for ocean-redox conditions and organic matter accumulation during the Cryogenian interglaciation. Palaeogeography, Palaeoclimatology, Palaeoecology, 563: 110169. doi: 10.1016/j.palaeo.2020.110169.

Tripathy G R, Singh S K. 2015. Re-Os depositional age for black shales from the Kaimur Group, Upper Vindhyan, India. Chemical Geology, 413: 63~72.

Uahengo C I, Shi X, Jiang G, Vatuva A. 2020. Transient shallow-ocean oxidation associated with the late Ediacaran Nama skeletal fauna: Evidence from iodine contents of the Lower Nama Group, southern Namibia. Precambrian Research, 343: 105732. doi: 10.1016/j.precamres.2020.105732.

van Acken D, Thomson D, Rainbird R H, Creaser R A. 2013. Constraining the depositional history of the Neoproterozoic Shaler Supergroup, Amundsen Basin, NW Canada: Rhenium-osmium dating of black shales from the Wynniatt and Boot Inlet Formations. Precambrian Research, 236: 124~131.

Wang Xiao, Li Yan, Li Yanzhang, Liu Yuwei, Duan Jianshu, Ding Hongrui, Wang Changqiu, Lu Anhui. 2018&. Effects of Mg^{2+} and SO_4^{2-} on Mn-carbonate mineralization induced by microorganisms in shallow seas. Earth Scinence——Journal of China University of Geosciences, 43(S1): 145~156.

Wang Dan, Zhu Xiangkun, Zhao Nina, Yan Bin, Li Xianhua, Shi Fuqiang, Zhang Feifei. 2019. Timing of the termination of Sturtian glaciation: SIMS U-Pb zircon dating from South China. Journal of Asian Earth Sciences, 177: 287~294.

Wang Jian, Li Zhengxiang. 2003. History of Neoproterozoic rift basins in South China: implications for Rodinia break-up. Precambrian Research, 122(1~4): 141~158.

Wang Ping, Algeo T J, Zhou Q, Yu W, Du Y, Qin Y, Xu Y, Yuan L, Pan W. 2019. Large accumulations of ^{34}S-enriched pyrite in a low-sulfate marine basin: The Sturtian Nanhua Basin, South China. Precambrian Research, 335: 105504. doi: 10.1016/j.precamres.2019.105504.

Wang Ping, Du Yuansheng, Yu Wenchao, Algeo T J, Zhou Qi, Xu Yuan, Qi Liang, Yuan Liangjun, Pan Wen. 2020. The chemical index of alteration (CIA) as a proxy for climate change during glacial—interglacial transitions in Earth history. Earth-Science Reviews, 201: 103032. doi: 10.1016/j.earscirev.2019.103032.

Wang Zhengjiang, Wang Jian, Jiang Xinsheng, Sun Haiqing, Gao Tianshan, Chen Jianshu, Qiu Yansheng, Du Qiuding, Deng Qi, Yang Fei. 2015&. New progress for the stratigraphic division and correlation of Neoproterozoic in Yangtze Block, South China. Geological Review, 61(1): 1~22.

Wang Fuliang, Fu Yong, Jiang Ran, Zhou Wenxi, Ge Zhihua, Wei Shuaichao, Liang Houpeng, Zhang Peng. 2016&. Research progress on Re-Os isotopes application in dating and paleoenvironmental interpretation during the Neoproterozoic to Early Cambrian Periods. Rock and Mineral Analysis, 35(5): 530~541.

Wang Jian, Liu Baojun, Pan Guitang. 2001&. Neoproterozoic rifting history of South China——Significance to Rodinia breakup. Mineralogy and Petrology, 21(3): 135~145.

Wang Xiaolei, Zhou Jincheng, Qiu Jiansheng, Gao Jianfeng. 2004&. Petrogenesis of Neoproterozoic peraluminous granites from northeastern Hunan Province: Chronological and geochemical constraints. Geological Review, 50(1): 65~76.

Wang Ziqiang, Gao Linzhi, Ding Xiaozhong, Huang Zhizhong. 2012&. Tectonic environment of the metamorphosed basement in the Jiangnan Orogen and its evolutional features. Geological Review, 58(3): 401~413.

Wang Wei, Cawood P A, Pandit M K, Xia Xiaoping, Raveggi M, Zhao Junhong, Zheng Jianping, Qi Liang. 2020. Fragmentation of South China from greater India during the Rodinia—Gondwana transition. Geology, 49(2): 228~232.

Wei Guangyi, Planavsky N J, He Tianchen, Zhang Feifei, Stockey R G, Cole D B, Lin Yibo, Ling Hongfei. 2021. Global marine redox evolution from the late Neoproterozoic to the early Paleozoic constrained by the integration of Mo and U isotope records. Earth-Science Reviews, 214: 103506. doi: 10.1016/j.earscirev.2021.103506.

Wei Guangyi, Wei Wei, Wang Dan, Li Tao, Yang Xiaoping, Shields G A, Zhang Feifei, Li Gaojun, Chen Tianyu, Yang Tao, Ling Hongfei. 2020. Enhanced chemical weathering triggered an expansion of euxinic seawater in the aftermath of the Sturtian glaciation. Earth and Planetary Science Letters, 539: 116244. doi: 10.1016/j.epsl.2020.116244.

Wei Shuaichao, Fu Yong, Liang Houpeng, Ge Zhihua, Zhou Wenxi, Wang Guangzhe. 2017. Re-Os geochronology of the Cambrian stage-2 and -3 boundary in Zhijin County, Guizhou Province, China. Acta Geochimica, 37(2): 323~333.

Wei Wei, Wang Dan, Li Da, Ling Hongfei, Chen Xi, Wei Guangyi, Zhang Feifei, Zhu Xiangkun, Yan Bin. 2016. The marine redox change and nitrogen cycle in the Early Cryogenian interglacial time: Evidence from nitrogen isotopes and Mo contents of the basal Datangpo Formation, northeastern Guizhou, South China. Journal of Earth Science, 27(2): 233~241.

Wu Chengquan, Zhang Zhengwei, Xiao Jiafei, Fu Yazhou, Shao Shuxun, Zheng Chaofei, Yao Junhua, Xiao Chaoyi. 2016. Nanhuan manganese deposits within restricted basins of the southeastern Yangtze Platform, China: Constraints from geological and geochemical evidence. Ore Geology Reviews, 75: 76~99.

Yamashita Y, Takahashi Y, Haba H, Enomoto S, Shimizu H. 2007. Comparison of reductive accumulation of Re and Os in seawater—sediment systems. Geochimica et Cosmochimica Acta, 71(14): 3458~3475.

Yang G, Hannah J L, Zimmerman A, Stein H J, Bekker A. 2009. Re-Os depositional age for Archean carbonaceous slates from the southwestern Superior Province: Challenges and insights. Earth and Planetary Science Letters, 280(1~4): 83~92.

Ye Yuntao, Wang Huajian, Zhai Lina, Wang Xiaomei, Wu Chaodong, Zhang Shuichang. 2018. Contrasting Mo—U enrichments of the basal Datangpo Formation in South China: Implications for the Cryogenian interglacial ocean redox. Precambrian Research, 315: 66~74.

Yeasmin R, Chen D Z, Fu Y, Wang J G, Guo Z H, Guo C. 2017.

Climatic—oceanic forcing on the organic accumulation across the shelf during the Early Cambrian (Age 2 through 3) in the mid—upper Yangtze Block, NE Guizhou, South China. Journal of Asian Earth Sciences, 134: 365~386.

Yin Chongyu, Wang Yangeng, Tang Feng, Wan Yusheng, Wang Ziqiang, Gao Linzhi, Xing Yusheng, Liu pPengju. 2006&. SHRIMP II U-Pb zircon date from the Nanhua Datangpo Formation in Songtao County, Guizhou Province. Acta Geologica Sinica, 80 (2): 273~278.

Yu Wenchao, Algeo T J, Du Yuansheng, Maynard B, Guo Hua, Zhou Qi, Peng Touping, Wang Ping, Yuan Liangjun. 2016. Genesis of Cryogenian Datangpo manganese deposit: Hydrothermal influence and episodic post-glacial ventilation of Nanhua Basin, South China. Palaeogeography, Palaeoclimatology, Palaeoecology, 459: 321 ~ 337.

Yu Wenchao, Algeo T J, Du Yuansheng, Zhou Qi, Wang Ping, Xu Yuan, Yuan Liangjun, Pan Wen. 2017. Newly discovered Sturtian cap carbonate in the Nanhua Basin, South China. Precambrian Research, 293: 112~130.

Yu Wenchao, Du Yuansheng, Zhou Qi, Peng Touping, Wang Ping, Yuan Liangjun, Xu Yuan, Pan Wen, Xie Xiaofeng, Qi Liang. 2016a&. Provenance of Nanhua Datangpo Formation manganese Mn deposit in Songtao area, East Guizhou Province: Evidence from Sr isotope. Earth Scinece, 41(7): 1110~1120.

Yu Wenchao, Du Yuansheng, Zhou Qi, Wang Ping, Qi Liang, Xu Yuan, Jin Song, Pan Wen, Yuan Liangjun, Xie Xiaofeng, Yang Bingnan. 2020&. Coupling between metallogenesis of the Cryogenian Datangpo-type manganese deposit in South China and major geological events, Journal of Palaeogeography (Chinese Edition), 22(5): 855~871

Yu Wenchao, Du Yuansheng, Zhou Qi, Wang Ping, Yuan Liangjun, Xu Yuan, Pan Wen, Xie Xiaofeng, Qi Liang, Jiao Liangxuan. 2016b&. LA-ICP-MS zircon U-Pb dating from the Nanhua Datangpo Formation in Songtao area, East Guizhou and its geological significance. Geological Review, 62(3): 539~549.

Yu Wenchao, Polgári M, Gyollai I, Fintor K, Szabó M, Kovács I, Fekete J, Du Yuansheng, Zhou Qi. 2019. Microbial metallogenesis of Cryogenian manganese ore deposits in South China. Precambrian Research, 322: 122~135.

Zhai Lina, Wu Chaodong, Ye Yuntao, Zhang Shuichang, Wang Yizhe. 2018. Fluctuations in chemical weathering on the Yangtze Block during the Ediacaran—Cambrian transition: Implications for paleoclimatic conditions and the marine carbon cycle. Palaeogeography, Palaeoclimatology, Palaeoecology, 490: 280 ~ 292.

Zhang Feifei, Zhu Xiangkun, Gao Zhaofu, Cheng Long, Peng Qianyun, Yang Dezhi. 2013&. Implication of the precipitation mode of manganese and ultra-high $\delta^{34}S$ values of pyrite in Mncarbonate of Xixibao Mn Ore Deposit in northeastern Guizhou Province. Geological Review, 59(2): 274~286

Zhang Qirui, Lan Zhongwu. 2016&. An update of the chronostratigraphy of the Nanhua system. Journal of Stratigraphy, 40(3): 297~301.

Zhang Sihong, Jiang Ganqing, Han Yigui. 2008. The age of the Nantuo Formation and Nantuo glaciation in South China. Terra Nova, 20 (4): 289~294.

Zhang Yujie, An Xianyin, Liu Shilei, Gao Yongjuan, Zheng Jie, Sang Yongheng. 2020&. The lithofacies, Mn-bearing sedimentary filling and paleogeographic pattern of Early Datangpo Stage and implied for manganese in the northeastern Guizhou Province. Geology in China, 47(3): 607~626.

Zhao Guochun, Wang Yuejun, Huang Baochun, Dong Yunpeng, Li Sanzhong, Zhang Guowei, Yu Shan. 2018. Geological reconstructions of the East Asian blocks: From the breakup of Rodinia to the assembly of Pangea. Earth-Science Reviews, 186: 262~286.

Zhao Junhong, Wang Wei, Liu Hang. 2015&. Geological evolution of the southeastern Yangtze Block during the Neoproterozoic. Bulletin of Mineralogy, Petrology and Geochemistry, 34(2): 227~233.

Zhao Yanyan, Zheng Yongfei. 2011&. Record and time limit of global Neoproterozoic Glaciation. Acta Petrologica Sinica, 27(2): 545~565.

Zhao Zhiqiang, Ling Yun, Li Heliang, Jiang Kai, Li Jie, Cai Keke, Liang Hong. 2019&. Geochemistry and significance of the Datangpo Formation in the Xiaochayuan manganese deposit in the Xiushan County, Chongqing. Bulletin of Mineralogy, Petrology and Geochemistry, 38(2): 330~341.

Zhou Chuanming, Huyskens M H, Xiao Shuhai, Yin Qingzhu. 2020. Refining the termination age of the Cryogenian Sturtian glaciation in South China. Palaeoworld, 29(3): 462~468.

Zhou Chuanming, Huyskens M H, Lang Xianguo, Xiao Shuhai, Yin Qingzhu. 2019. Calibrating the terminations of Cryogenian global glaciations. Geology, 47(3): 251~254.

Zhou Chuanming, Tucker Robert, Xiao Shuhai, Peng Zhanxiong, Yuan Xunlai, Chen Zhe. 2004. New constraints on the ages of Neoproterozoic glaciations in south China. Geology, 32(5): 437~440.

Zhu Bi, Becker H, Jiang Shaoyong, Pi Daohui, Fischer-Gödde M, Yang Jinghong. 2013. Re-Os geochronology of black shales from the Neoproterozoic Doushantuo Formation, Yangtze platform, South China. Precambrian Research, 225: 67~76.

Zhou Qi, Du Yuansheng, Qin Ying. 2013&. Ancient natural gas seepage sedimentary-type manganese metallogenic system and ore-forming model: A case study of Datangpo-type manganese deposits formed in rift basin of Nanhua Period along Guizhou—Hunan—Chongqing bounder area. Mineral Deposits, 32(3): 457~466.

Zhou Qi, Du Yuansheng, Yuan Liangjun, Zhang Sui, Yu Wenchao, Yang Shengtang, Liu Yu. 2016&. The structure of the Wuling rift basin and its control on the manganese deposit during the Nanhua Period in Guizhou—Hunan—Chongqing border area, South China. Earth Science, 41(2): 177~188.

Zhu Xiangkun, Peng Qianyun, Zhang Renbiao, An Zhengze, Zhang Feifei, Yan Bin, Li Jin, Gao Zhaofu, Qin Ying, Pan Wen. 2013&. Geological and geochemical characteristics of the Daotuo super large manganese ore deposit at Songtao Country in Guizhou Province, South China. Acta Geologica Sinica, 87(9): 1335~1348.

Zou Guangjun, Huang Jianzhong, Ling Yuexin, Tan Shimin, Cao Chuanghua, Huang Gefei, Wen Chunhua. 2020&. Lithofacies paleogeography and sedimentary evolution of Hunan—Guizhou—Chongqing border area in the Nanhua Period. Acta Geoscientica Sinica, 41(2): 207~218.

Metallogenesis and mineralization backgrounds of Neoproterozoic Cryogenian manganese deposits in Nanhua Basin

FU Yong[1, 2)], GUO Chuan[1, 2)]

1) *The College of Resources and Environmental Engineering*, *Guizhou University*, *Guiyang*, 500025;

2) *Key Laboratory of Karst Georesources and Environment*, *Ministry of Education*, *Guizhou University*, *Guiyang*, 500025

Objectives: The Neoproterozoic Cryogenian Datangpo manganese of the Nanhua Basin that was formed after Cryogenian Sturtian glaciation has been one of the major manganese production sites, the mineralization backgrounds and development mechanism of which have received much more attention. The initiation and termination ages of the Sturtian glaciation and the mineralization ages of the Datangpo manganese deposits, the architectural evolution of the Nanhua Basin, the weathering intensity and climatic conditions, and the formation mechanism of the Cryogenian manganese deposits were reviewed.

Methods: This paper systematically summarized the commence and termination ages of the Sturtian glaciation elsewhere around the world, the tectonic architecture of the Nanhua Basin and the paleoclimate evolution during the deglaciation of the Neoproterozoic Cryogenian; meanwhile. the causal relationship between the metallogenesis of depositional manganese deposits of the Nanhua Basin and the aforementioned major geological events were comprehensively documented.

Results: The Sturtian glaciation of the Nanhua Basin initiated at ~ 717 Ma and terminated before ~ 660 Ma. The syndepositional fault-controlled horst and graben subbasins were formed in the interior of the Nanhua Rift Basin. The weathering indices such as chemical index of alteration (*CIA*), Li isotope (δ^7Li) and Os isotopic composition ($n(^{187}Os)/n(^{188}Os)$) are indicative of a cold and arid climate of the Nanhua Basin during the late Sturtian glaciation to early interglacial Datangpo Age. The climatic condition changed into a warm and humid climate, quickly returned into a cold and arid climate until the middle to late Datangpo Age, and then transited into a warm and humid climate that persisted into late Datangpo Age. The surface seawater of the Nanhua Basin was well oxygenated after the Sturtian glaciation; meanwhile, the deep water was dominated by anoxia with intermittently oxic condition.

Conclusions: The initiation and termination of the Sturtian glaciation of the Nanhua Basin took place most likely synchronously with elsewhere around the world. The mineralization timing of the Cryogenian Datangpo manganese deposits likely developed before ~ 660 Ma. The hydrothermal fluids provided considerable amounts of metallogenesis materials for the Datangpo manganese deposits and dictated their developments, which were precipitated, and were accompanied by organic matter burial and microbe-mediated to transferred into rhodochrosite during early diagenesis.

Keywords: Sturtian glaciation, paleoclimate, Datangpo manganese deposits, Neoproterozoic, Nanhua Basin

Acknowledgements: This study was supported by National Natural Science Foundation of China (Nos. 41763006 and 41673060), the project of "Geology of mineral resources in China" from China Geological Survey (No. DD20190379) and Talent Base Project of Guizhou Province (No. RCJD2018-21)

First author: FU Yong, male, born in 1980, Ph. D., associate professor, mainly engaged in sedimentology, sedimentary geochemistry and sedimentary deposit science; Email: byez1225@126.com

Manuscript received on: 2021-03-15; Acceptedon: 2021-05-28; Network published on: 2021-06-20

Doi: 10.16509/j.georeview.2021.06.031　　**Edited by**: LIU Zhiqiang